THESIS FOR THE DEGREE OF DOCTOR OF PHILOSOPHY
IN SOLID AND STRUCTURAL MECHANICS

Thermomechanics of tread braking

Braking capacity of railway wheels

ERIC VOORTMAN LANDSTRÖM

Department of Mechanics and Maritime Sciences
Chalmers University of Technology
Gothenburg, Sweden, 2024

Thermomechanics of tread braking

Braking capacity of railway wheels

Eric Voortman Landström
ISBN 978-91-8103-150-8

Doktorsavhandlingar vid Chalmers tekniska högskola
Ny serie nr 5608
ISSN 0346-718X

Department of Mechanics and Maritime Sciences
Chalmers University of Technology
SE-412 96 Gothenburg, Sweden
Phone: +46 (0)31 772 1000

Cover:
Thermographic image of a tread braked wheel during braking

Printed by Chalmers Reproservice
Gothenburg, Sweden, December 2024

If you do things right, people won't
be sure you've done anything at all.
God Entity, Futurama, "Godfellas" (S03E20)

Thermomechanics of tread braking

Braking capacity of railway wheels

Eric Voortman Landström
Department of Mechanics and Maritime Sciences
Chalmers University of Technology

Abstract

Tread brakes are the most common type of railway braking system, wherein a block of friction material is pushed onto the rolling surface, or 'tread', of a railway wheel. Although simple, inexpensive, and maintenance-efficient, a complex thermomechanical loading situation occurs, in which the elevated temperatures from the frictionally dissipated energy interact with wheel-rail rolling contact loads. This may cause damage to the wheels and other components, resulting in disruptive and costly maintenance procedures. In severe cases, it could lead to wheel failure and derailment.

The aim of this thesis is to determine thermomechanical limits of the tread braking system and to find in which situations the wheel and brake experience damage which exceeds safe or economical limits or fail entirely. In addition, it aims at presenting models capable of accurately simulating the dimensioning or critical loading cases. To achieve this, knowledge building based upon experimental campaigns and numerical simulations has been made.

The temperature field around the wheel has been studied in full-scale experiments and in–field conditions. Results from these studies show that the temperature field has the potential to form severe long-wavelength non-uniformities, which have the potential to induce increased levels of residual stresses in the wheel. The thermal degradation experienced by the pearlitic steel is shown to significantly affect the mechanical strength of the material, causing plastification in the rolling surface.

The numerical work has focused on both calibrating a finite element material model to accurately and stably model the behaviour seen in experiments and then employing it to study the braking scenarios envisioned. Both simulations of tread braking at high brake loads and rolling contact at elevated temperatures are studied in the thesis.

Keywords: Railway wheels, tread braking, thermomechanics, finite element analysis, full-scale testing, material modelling

Blockbromsningens termomekanik
Bromskapacitet hos järnvägshjul
Eric Voortman Landström
Mekanik och Maritima Vetenskaper
Chalmers Tekniska Högskola

Sammanfattning

Blockbromsning är det vanligaste bromssystemet på järnvägsvagnar, och fungerar genom att ett block av friktionsmaterial trycks mot hjulets löpbana, dvs den yta som rullar på rälsen. Det är ett enkelt, billigt och underhållseffektivt system, men en komplicerad termomekanisk situation uppstår när höga temperaturer från friktionsvärmen interagerar med rullkontaktkrafterna mellan hjul och räls. Det kan orsaka skador på hjul och andra komponenter, som i sin tur leder till störande och dyra underhållsåtgärder. I svåra fall kan det även leda till hjulhaveri och urspårningar.

Syftet med denna avhandling har varit att bestämma de termomekaniska gränserna för blockbromsningssystemet och lastfallen där hjul och broms skadas bortom säkra eller ekonomiska gränser eller havererar. Dessutom är ett mål att presentera modeller som kan simulera de dimensionerande eller kritiska lastfallen. En kombination av experiment, fältmätningar och numeriska analyser har utförts för att uppnå detta.

Temperaturfältet runt hjulet har studerats i fullskaleexperiment och i fält. Resultaten från dessa mätningar visar att bromsarna i vissa fall orsakar långvågiga temperaturojämnheter i omkretsled, som påverkar restspänningsfältet i hjulet och kan leda till brott. Mätningar påvisar även att materialnedbrytningen på grund av höga temperaturer orsakas en permanent försvagning av hjulmaterialet, vilket i sin tur också ökar skadorna på löpbanan.

Det numeriska arbetet har fokuserat på att kalibrera finita elementmodeller för hjulmaterialet för att tillförlitligt och stabilt kunna modellera materialbeteendet som ses i tester. Modellerna har sedan tillämpats i simuleringar av bromsfall. Framför allt bromsningar vid höga temperaturer och vid rullkontakt har undersökts i denna avhandling.

Nyckelord: Järnvägshjul, blockbromsning, termomekanik, finit elementanalysis, fullskaletester, materialmodellering

List of Publications

This thesis is based on the following publications:

[A] **Eric Voortman Landström**, Erika Steyn, Johan Ahlström, Tore Vernersson, "Thermomechanical testing and modelling of railway wheel steel". *International Journal of Fatigue*, Volume 168, 107373, March 2023.

[B] **Eric Voortman Landström**, Tore Vernersson, Roger Lundén, "Improved modelling of tread braked wheels using an advanced material model". *Proceedings EuroBrake 2022*, May 2022..

[C] **Eric Voortman Landström**, Tore Vernersson, Roger Lundén, "Analysis and testing of tread braked railway wheel — Effects of hot spots on wheel performance". *International Journal of Fatigue*, Volume 180, 108116, March 2024.

[D] **Eric Voortman Landström**, Tore Vernersson, Roger Lundén, "Characterisation and Evaluation of Global Uneven Heating during Railway Tread Braking – Brake Rig Testing and Field Study". *To appear in IMechE part F: Journal of Rail and Rapid Transit.*

[E] **Eric Voortman Landström**, Matheus de Lara Todt, Tore Vernersson, Roger Lundén, "Non-uniform temperature and residual stress effects during railway tread braking". *Revised version to be submitted for international publication.*

[F] **Eric Voortman Landström**, Ryo Ozaki, Kazuyuki Handa, Tore Vernersson, "Thermomechanical Contact Behaviour of Tread Braked". *Revised version to be submitted for international publication.*

[G] **Eric Voortman Landström**, Tore Vernersson, "Numerical study of rolling contact fatigue at tread braking conditions". *Revised version to be submitted for international publication.*

Other publications by the author, not included in this thesis, are:

[H] **Eric Voortman Landström**, Tore Vernersson, Roger Lundén, “Improved Finite Element Modelling of Tread Braked Wheel Performance Verified by Brake Rig Tests”. *Proceedings 20th International Wheelset Congress*, May 2023, Chicago, IL (USA).

[I] Robin Rydbergh, Lisa-Marie Witte, Jonas Sjöblom, Nathalie Scheers, Amir Saeid Mohammadi, **Eric Voortman Landström**, Tore V Vernersson, Per Malmberg, “ToF-SIMS analyses of brake wear particles in human epithelial Caco-2 cells”. *To appear in Journal of Aerosol Science.*

[J] Kazuyuki Handa, Ryo Ozaki, **Eric Voortman Landström**, “Safety Assessment of Tread-Braked Railway Wheels Under Malfunction Drag Braking Using Ultrasonic Acoustoelasticity”. *Proceedings the 31st Railway Technology Joint Symposium*, November 2024, Tokyo, (Japan). In Japanese. Original title: 超音波音弾性による踏面ブレ ーキ不緩解時の車輪安全性判定手法.

Acknowledgments

In his work *Devotions upon Emergent Occasions* (1624), John Donne wrote the poem *No man is an island*, beginning with the stanza

No man is an island,
Entire of it self,
Every man is a piece of the continent,
A part of the main.

Although the poem itself explores human connection and loss, the first part is rather fitting here as well. This work would not have been possible without the assistance and cooperation of numerous colleagues and friends, whose contributions have become part of the main. The following acknowledgements list only some of them, but I remember you all.

This work was performed during 2020–2025 at the Division of Dynamics at the Department of Mechanics and Maritime Sciences, Chalmers University of Technology. It is part of project SD11 “Tread braking – capacity, wear and life” within the Swedish National Centre of Excellence in Railway Mechanics CHARMEC (CHAlmers Railway MEChanics). The special support from Lucchini (in Sweden and Italy), Wabtec Faiveley Nordic, Becorit GmbH, LKAB/Malmtrafik AB, from Trafikverket’s Areas of Excellence, from the European Programmes Shift2Rail and Europe’s Rail and the project reference group with members from Alstom (in Sweden, Germany and UK), Green Cargo, Systra Sverige and Wabtec Faiveley Nordic is gratefully acknowledged. The computations were enabled by resources provided by Chalmers e-Commons at Chalmers.

Perhaps the most important acknowledgement goes to two people, without whose work this thesis would not have become a reality, Docent Tore Vernersson and Professor Roger Lundén. Your guidance, knowledge, network and stoic proofreading, have made this work what it is. In addition to these, I also want to express my deepest gratitude to Mr Jan Möller for his participation in designing and assembling the Chalmers brake roller rig. Additionally, I want to thank Dr Erika Steyn and Professor Johan Ahlström for the good collaboration on Paper A. Your support was important for the initial work performed, and the excellent experiments helped immensely.

I also want to express my deepest gratitude to my more faraway colleagues, Dr Handa Kazuyuki, Mr Ozaki Ryo, Dr Matsui Motohide and all of my colleagues from the Friction Materials Laboratory at 鉄道総研 (RTRI) in Tokyo, Japan, for welcoming me. From the sun rising over the Seto sea, to the stars at night sky of Kamikōchi, Japan has truly been the experience of a lifetime, and I am longing to come back and continue our work. From another part of the world, I also want to thank Mr Andrea Ghidini and Mr Lorenzo Ghidini at Lucchini RS SpA for their friendship and collaboration throughout the project. I look forward to more years collaboration, hiking, Swedish pizza and turtles.

Furthermore, I would to thank all of my current and previous colleagues at Chalmers, both at M2 and at IMS. A special acknowledgement to my "kontorssambo" Henrik Vilhelmson, who somehow managed to survive the ordeal of sharing an office with me. In addition, I want to thank my fellow PhD students, including Kim, Carolyn, Michele, Ata, Kourosh, *The Bangalore Torpedo* and many, many more, both old and new, who made floor 3 an amazing place.

And then, the largest group. I want to express my deepest gratitude to all the students I have had the opportunity to interact with during these five years at Chalmers. It has been an honour and a privilege to be your teacher and your friend, both inside and outside the classroom. There are far too many of you even to attempt to list but know that the students at Maskinteknologsektionen have made these past several years magical. Shine on you crazy diamonds.

Finally, I also want to thank my family, who have supported me during all of these years at university, whether it has been during my time at KTH in Stockholm or far beyond Sweden, as well as the friends who have been there all along. Some even moved here to Gothenburg, much to my surprise.

It is, as they say, that the real treasure was the friends we made along the way.

Göteborg, December 2024
Eric Voortman Landström

Preface

Originally, my suggested title was 'Treads breaking', as a play on the overall subject of *tread braking* and that finding the limits when these rolling surfaces would break was one aim of the project. This playful suggestion was, as might be expected, immediately rejected by the powers that be and in the end it was a moot point as no treads were actually broken. In one sense, this highlights the resilience of the wheel system in that no failure occurred at testing despite combined loads significantly above normal levels. At one point, a hacksaw was applied to a thoroughly tested wheel and yet still it refused to fracture. The wheel finally yielded when it was cut by electric discharge machining.

It also shows the current issues of testing, as unexpected results still occur despite our best experimental efforts. The discrepancy is likely due to a manifold of reasons, but one probable is simply the fact that there are further variables in actual service, concerning maintenance, brake adjustments, and loading histories, along with a host of other reasons owing to the pure statistical distribution of material quality. The topic itself has been studied from many angles, both theoretical and practical, for several decades at this point, and although improvements have been made, it is still difficult to predict and model what happens in the interfaces of the wheel–brake–rail system.

Knowing the limits of the tread braking system and whether it could be safely utilised in scenarios beyond the current regulatory limits would be beneficial for the railway industry. Most of the braking effort in high-speed trains is carried by electrodynamic brakes rather than mechanical friction brakes. Today, these are normally fitted with disc brakes, which is positive in the sense that the wheel rolling surface is not heated, although significant unsprung mass is added to the wheelset. Allowing tread brakes would however provide a simpler and inexpensive alternative, and it is not necessarily unrealistic given improvements in wheel design and materials over the last decades, in particular if frictional braking capacity is only rarely required. There is currently ongoing work by others to investigate the possibility of extending the service envelope of tread brakes, which this work may aid in.

The primary results of the work performed as part of this thesis provide one more stone on the road to understanding and improving the usage of the tread braking system, but it should not be considered exhaustive. The experimental results from Gothenburg, Narvik and Tokyo coupled with the numerical work will hopefully serve a good purpose in the future.

Contents

E

F

G

Part I

Extended Summary

CHAPTER 1

Introduction

Railways are in one sense the mode of transport that ushered in the modern age of transportation, utilising the potential that came from effective rolling and the steam engine. To remain competitive in an age of air and road travel, it is desirable to achieve both higher speeds and higher axle loads, which in turn increases the operational demands on the braking system. Given that braking requirements are one of the ultimate limits of railway capacity, it is desirable to fully understand the service envelope of the braking system so that it can be best utilised in a safe and maintenance-efficient way.

For tread brakes, which are commonly used on freight vehicles, trams, subways, narrow-gauge railway vehicles and also on some passenger trains, modern requirements on noise emissions mandate thermally less optimal brake block materials, which in turn may have the propensity of increasing wheel damage. It is therefore of importance to have full knowledge of the service envelope for the braking system so that it can continue to be broadly used in a safe and maintenance-efficient way.

In this chapter, the background and motivation is presented in Section 1.1, the aim and limitations are presented in Section 1.2, the collaborations are presented in Section 1.3 and in Section 1.4 an outline of the thesis is given.

1.1 Background and motivation

Although overland rail freight volumes have long been surpassed by road freight volumes [1], modern-day environmental awareness may lead to somewhat of a renaissance of railway operations. They present transport opportunities with less environmental impact due to lower rolling resistance, widespread electrification and longer-lasting vehicles compared to automotive transports [2]. This however raises the demands of shorter travel times, high reliability and low cost in combination with increased traffic volumes to provide economic incentives as well as to maintain safety. As noted in several major derailments within the last few years [3–5], limitations of network capacity quickly result in significant economic losses. Reliability of traffic is thus a major concern for stakeholders. The ability to predict damage to optimize maintenance procedures and prevent component damage or derailments is of significant importance for the future of the railway freight industry. In addition to this, increased axle loads and longer trains are long-standing requests from operators [6].

All of these factors put increased requirements on the braking system, which is one of the critical components with regard to the reliable and safe operations of trains.

Modern braking systems are often a combination of electrodynamic (ED) brakes and mechanical brakes in the form of tread (block) brakes or disc brakes, together with supplementary braking systems such as magnetic track brakes or eddy current brakes. An overview of the brake system hierarchy is shown in Figure 1.1. Freight trains such as the iron ore trains in northern Sweden and Norway, pictured in Figure 1.2 as well as low-speed and narrow-gauge trains, exemplified in Figure 1.3, are predominately equipped with tread brakes that are the focus of the present work.

Ideally, ED brakes, either resistive or regenerative, serve as the primary brakes as they allow the transformation of kinetic energy into either thermal energy on the braking resistor or electrical energy fed back into the overhead catenaries. They have the benefit of not causing any wear comparable to the contact in the mechanical brake, increasing the life of the rotor (wheel/disc) and friction material (block/pad), as well as reducing costs through the feedback of electrical energy into the grid for regenerative braking. Limitations are however that, depending on the type of train, the braking force generated by the ED brake may be relatively low, particularly at low speeds due to

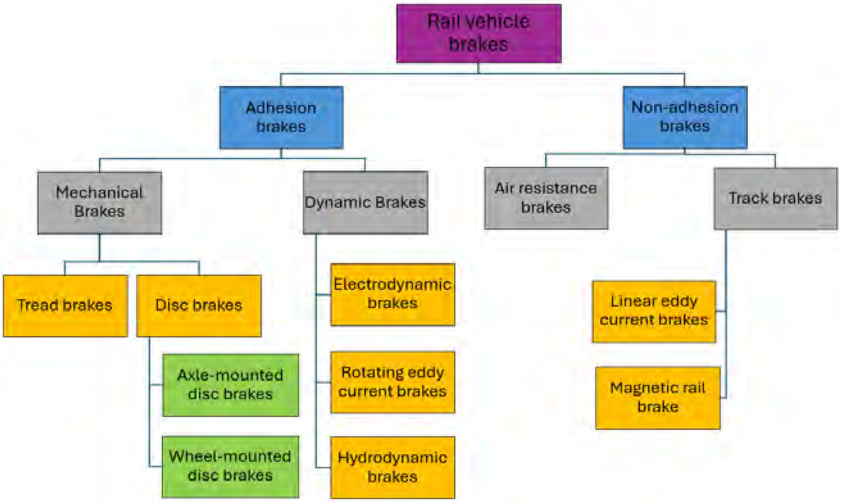

Figure 1.1: Categorization of rail vehicle braking systems.

Figure 1.2: LKAB Iron ore train on the Swedish iron ore line. This is currently the most heavily laden train line in Europe with regards to axle load, with an axle load limit of 31,5 tons. As with most freight cars, the iron ore wagons are equipped with tread brakes.

Figure 1.3: Keihan 800 series electric multiple unit (EMU) commuter train in Biwako-Hamaōtsu, Kyoto, Japan. This specific model, in use on the Keihan Keishin-line, is designed for mountain railways due to the gradient between Kyoto city and Biwako-Hamaōtsu. It is the only Japanese example of a commuter train with cast iron brake blocks.

the deficiency of the traction motors to then act as a generator [7]. In cases where the ED brakes either provide insufficient capacity or are malfunctioning, the friction brakes are nonetheless required to provide sufficient braking effort to safely brake the train. It is therefore of high importance to be able to predict the functioning of the mechanical braking system. It should be noted that even very novel train concepts such as the in Japan currently under construction *Linear Chuo Shinkansen* (リニア中央新幹線), which utilises an electrodynamic suspension system (i.e. magnetic levitation), still requires friction brakes (wheel-mounted disc brakes) for the portion of travel conducted at low speeds [8].

Freight trains generally lack any electrical system at all apart from the locomotive itself, which either draws power from overhead catenaries or generates it via an alternator. For these trains, mechanical brakes are the only option for the wagons. Additionally, for heavy haul trains such as the iron ore trains in northern Sweden, feedback capacity may be limited or the driver may prefer to use friction brakes wholly or in conjunction with ED brakes, as can be seen on the descending route on the Ofoten line from Riksgränsen to Narvik. In this case, friction brakes are required as a backup in case of loss of overhead power or to supplement (in some cases fully) the ED brakes. In light of the fact that prolonged braking applications ('drag braking') on long descents are generally more damaging to the wheels than the shorter but more intense stop braking applications, it is of high importance to determine the allowable service envelope to prevent damage.

In this thesis, the main focus has been on expanding the knowledge with respect to the thermomechanical aspects of the tread braking system. The aim of the studies has been to investigate various phenomena related to tread braking (heat transfer, material mechanics, rolling contact fatigue). The results have been achieved through a combination of laboratory testing, full-scale brake dynamometer testing (both stop and drag braking) and field measurements on freight lines as well as modelling and numerical simulations of both stop and drag braking applications. The present thesis is a continuation of the work performed in CHARMEC projects *SD1*, *SD4*, *MU21*, *SD7*, *SD10* and *MU32* [9], and can be considered a stepping stone on the way to fully understanding the tread braking system.

1.2 Aim of thesis

The main goal of the thesis has been to determine the thermomechanical limits of the tread braking system so that it can be utilised broadly in a safe and maintenance-efficient way. Knowledge building has been based upon a combination of numerical simulations and experimental campaigns (specimen testing, full-scale and field testing) to determine how thermal and mechanical damage occurs in a wheel. Using data from the experimental trials, numerical thermal and mechanical models can be calibrated and extended to simulate the combined braking-rolling process for tread braked wheels in the areas of high-temperature material behaviour, thermomechanical fatigue and rolling contact. To this end, several different studies have been performed within the scope of this thesis, summarised as follows:

- Calibration and extensions of wheel steel material models based upon isothermal and anisothermal mechanical experiments with the expected temperature range of 20 – 650 °C was studied in **Paper A**. The range was then extended to 750 °C in **Paper C**.

- The temperature field on the wheel rolling surface is investigated in detail using radiometric methods in **Paper C**, **Paper D** and **Paper F**. A methodology to study the temperature non-uniformities that occur are developed in **Paper E** and **Paper F**. Furthermore, verification of the occurrence of non-uniform heating in field conditions is performed in **Paper D**.

- Investigation of high temperature rolling contact fatigue in a wheel–brake–rail–system is made in **Paper F**. Using results from a full-scale brake dynamometer and a brake roller rig, it has been possible to study the dominating phenomena during high temperature rolling contact.

- Simulations of the thermomechanical loading process are presented in **Paper B**, **Paper D** and **Paper E**. The inclusion of rolling contact damage has been simulated in **Paper G**.

A flowchart is presented in Figure 1.4, illustrating how the appended papers are connected.

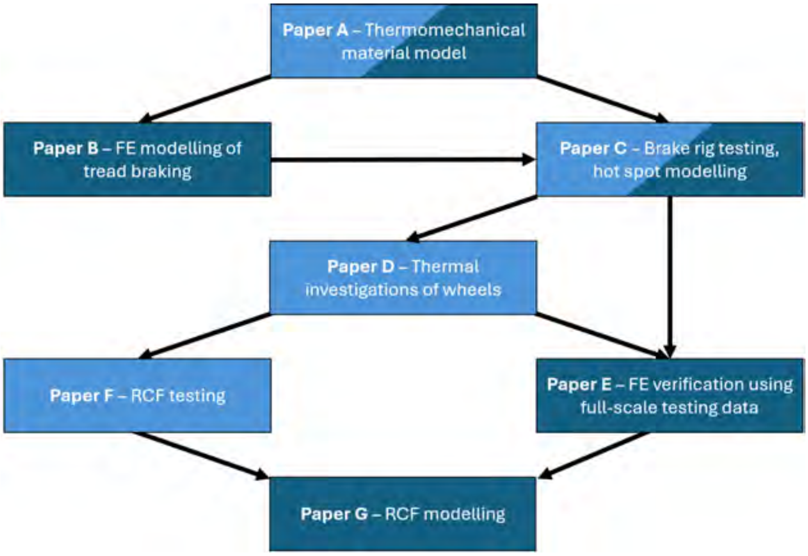

Figure 1.4: Flowchart of how the research papers are connected

Limitations

Due to the limited availability of performing experiments and the highly non-linear nature of the numerical work, the following limitations are used:

- All experimental work that also studies mechanical effects is performed in laboratory environments instead of field conditions.
- The frictional heating can be considered sequentially coupled from the mechanical simulations rather than fully coupled. This means that the thermal problem is solved independently of the mechanical one, and then used as input data for the mechanical problem, rather than solving the entire thermomechanical problem in one simulation.
- Only macro-scale effects are considered, with micro-scale material phenomena such as spheroidisation being approximated by higher-level functions.
- ER7 wheel steel is the only material studied in the thesis.

- Only a few specific wheel geometries are considered, primarily Swedish or European designs. All wheels are at or close to the wear limit.

1.3 Research Collaboration

The work performed in this thesis has been carried out within the CHARMEC project SD11 *Tread braking - capacity, wear and life.*

The experimental materials testing and characterisation from **Paper A** were carried out in collaboration with Dr Erika Steyn and Professor Johan Ahlström working within the CHARMEC project MU36 *Material Characteristics in welding and other local heating events* at Chalmers Industrial and Materials Science. In Project MU36, thermomechanical and hardness testings of wheel steel specimens were performed to gather the data used in the material model enhancements and in the calibration process performed in the present work.

The thermal simulations performed in **Paper E** were carried out in collaboration with Mr. Matheus de Lara Todt working within the CHARMEC project SD12 at Chalmers Mechanics and Maritime Sciences.

The stop braking tests performed in **Paper F** were carried out in collaboration with Dr. Handa Kazuyuki and Mr. Ozaki Ryo at Friction Materials Division of the Materials Technology Department at the Railway Technical Research Institute (RTRI) of Japan.

1.4 Outline of thesis

The extended summary of this thesis is structured in the following manner:

- In Chapter 2, an overview of the tread braking system is presented. Current regulations and requirements within the Swedish and European Union framework are given. The different designs and employed brake block materials are presented, as well as a historical outlook of the tread braking system.

- Chapter 3 presents the frictionally induced thermal effects at tread braking and shows how the wheel is affected by the frictional work performed during brake operations. Various phenomena such as uneven heating, thermoelastic instabilities and contact evolution are shown together with measurement and modelling methods.

- Chapter 4 continues building upon the thermomechanics by introducing the mechanical coupling that occurs when the wheel is heated during the brake applications. This chapter also discusses the effect of thermal damage on the material, as well as the effects of the elevated temperatures on the rolling contact and wear.

- Chapter 5 then goes into the modelling aspects and finite element implementation, optimisation and validation procedures used in addition to discussing potential avenues of improvement and alternatives.

- Chapter 6 describes the experimental methods and equipment used in the thesis, with an additional overview of the types of testing machines that are in use in general, and in the present work specifically.

- A summary of the appended papers is given in Chapter 7.

- The conclusions drawn from the work performed during the course of this thesis are presented Chapter 8.

- Ideas for possible future research that continues the work performed in this thesis are listed in Chapter 9, with some mentions of ongoing work.

CHAPTER 2

Overview of the tread braking system

This chapter introduces the tread braking system, also known as the 'block braking system'. These two expressions will be used interchangeably in the rest of this thesis. The chapter aims to explain how the system functions, including its benefits and drawbacks, compared to alternatives and complementary systems. Regulations and standards governing its functionality are presented for the overall system and for the wheel and the brake block. Finally, a historical overview is given, summarising the evolution of the tread braking system from its inception in the latter half of the 19th century to today.

2.1 Introduction

Block braking is the most commonly used braking system for freight wagons in the world. It is also the most commonly used *frictional* braking system for subways, light rail systems and also for narrow-gauge railway vehicles due to the difficulties in mounting disc brakes on the short axles. The operational principle is to dissipate the kinetic or potential energy of the train via the frictional work performed between the brake block and the wheel running surface ('tread'), see Figure 2.1. This frictional work is then transformed into thermal energy, partitioned between the block(s) and the wheel. After this, the energy is further conducted into the rail via the wheel, the block holder via the brake block as well as to the axle, the bearings and the general environment through convection and radiation. There are also some variations of the arrangement, with different numbers of blocks mounted on each wheel, detailed in Figure 2.2.

The tread braking system is attractive for several reasons [7]:

- **Low complexity** as it is externally mounted on the bogie frame, requiring little adaptation of wheels and axle.
- **Low-cost** due to the relative simplicity of the system.
- **Low spatial requirements** as the actuator does not require space on the wheelset, which may be an issue for disc brakes, as well as adding no unsprung mass.

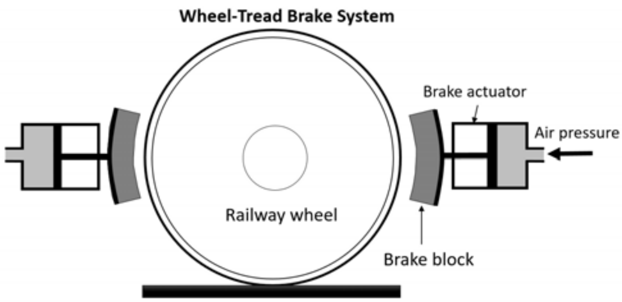

Figure 2.1: Schematic drawing of the tread braking system.

- **Straightforward and easy maintenance** as the external mounting makes access relatively simple. Maintenance of brake discs preferably be synchronised with maintenance of wheel for good economy, whereas blocks can be removed outside scheduled maintenance sessions.

- **Improved adhesion** between wheel and rail, as the tread brake can clean and roughen the wheel rolling surface.

- **Improved short-circuiting of rails** for the proper functioning of the signalling system.

The attractiveness of the system is balanced by the fact that the brake block interacts directly with the wheel rolling surface, resulting in heating and wear of wheel treads. Modern fully laden freight trains require significant braking capacities, with for example the iron ore trains between Riksgränsen and Narvik needing an average of 20 to 30 kW of continuous braking power per wheel for the approximately 40 min, 43 km descent. Furthermore, the CEN standards on wheel dimensioning [11, 12] calls for a brake testing verification

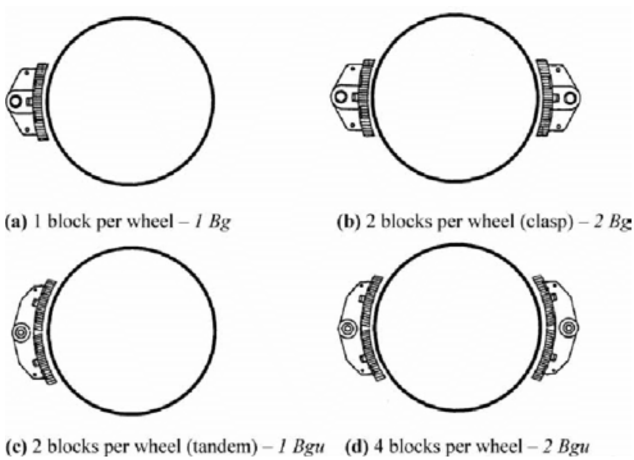

Figure 2.2: Four common block arrangements. (a) Single block, (b) Two blocks in clasp, (c) two blocks in tandem, (d) four blocks in two tandem arrangement. *Bg* and *Bgu* stands for 'Bremsklotz geteilt' and 'Bremsklotz geteilt underteilt', respectively [10].

using 50 kW for 45 min. This represents a substantial amount of frictionally dissipated energy, which causes considerable heating to both the brake block and the wheel, which will rapidly heat the surfaces in contact. The interaction between the wheel and brake causes a complex thermomechanical loading situation due to the potentially very intense thermal loads on the area of the wheel that is also exposed to very high contact loads from the rail. This sets a limit on safe braking. Too high temperatures and the wheel will suffer permanent damage as the material deteriorates in addition to residual stresses exceeding regulatory limits. In turn, these could cause wheel failure when combined with cracks initiated during rolling contact. Because of the potential damage to the track and other components and the risk of injuries to passengers and cargo, there is a very real need to ensure that the braking limits of wheels are well understood.

The overall requirements on train braking performance are governed by either national [13, 14] or international regulations for railways. The intention is to regulate braking distance so that there is always sufficient space for one train to fully decelerate to avoid collisions [7] or stop within regulated distances. This distance is then limited by braking capacity, which in turn is limited by both considerations for the wheel and train (e.g. avoid damage to components) as well as the passengers (as extremely high decelerations may cause discomfort or injuries). For trains in general, it should be noted that the braking distance is generally longer than the actual sight distance because of the low adhesion between wheel and rail, which is why the signalling system is of such importance. Knowing the limits of the braking system is therefore of utmost importance as it can then be utilised to its full extent, as ultimately, the capacity of the railway system is dependent on accurate braking performance and components that work predictably. Additionally, any increases in e.g. speed or loading limits would have to be coped by the braking system so that braking distances can be maintained. Examples of two braking sequences as calculated by the European Train Control System (ETCS) [15], one for a passenger train and one for a heavy haul train based on the Iron ore train, are shown in Figure 2.3.

The current speed limit of trains using tread brakes is 160 km/h in Europe and 130 km/h in Japan, with some countries allowing higher in specific circumstances. This is however for passenger trains, with freight trains being limited to lower speeds due to higher axle loads. There is some interest

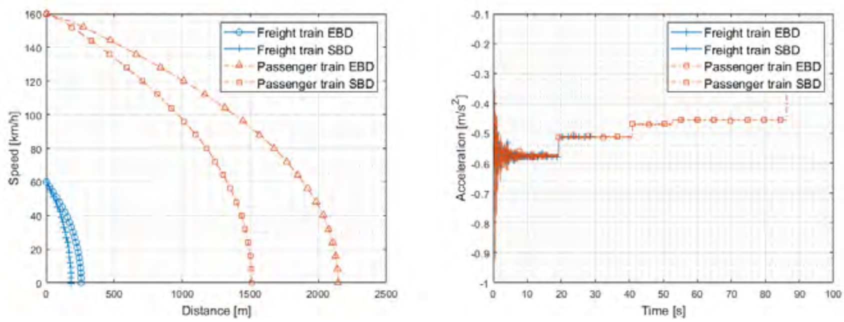

(a) **(b)**

Figure 2.3: ERTMS braking curves as calculated for service braking deceleration (SBD) and emergency braking deceleration (EBD) for both freight trains (in blue, v_0 = 60 km/h) and passenger trains (in red, v_0 = 160 km/h). a) Speed vs distance and b) estimated acceleration vs time. Note the overlapping of the curves.

in raising these speed limits [16–18], which would require increased braking performance and thus exacerbate the need for actually determining the thermomechanical limits. Some results in this thesis suggest that this may be thermomechanically reasonable for stop braking using sintered or composite blocks, but surface cracks can initiate even after only a few severe stop braking cycles [19] without proper system knowledge. In another sense, however, this remains an issue in theory only as the effective speed of railway freight is significantly lower in practice due to other factors [20]. Nonetheless, allowing tread brake systems on moderately high-speed passenger lines (e.g. up to 200 km/h) may provide an attractive alternative compared to the more expensive disc brakes. Increased speeds on freight trains may improve the overall network throughput due to more similar train speeds in mixed traffic.

2.2 Historical Overview

The earliest forms of train brakes, introduced in the 1830s, were manually activated through beams or screws [21], with the braking being generally limited by how quickly the brake porters could set them in place after being given an auditory braking signal. Over the following decades, several different mechanisms were attempted with various degrees of success [22], usually being limited by the train length, sensitivity to damage or overall complexity. The first generation of air brakes using a compressor on the locomotive were more efficient than manual brakes, but were sensitive to brake line ruptures and required lengthy pump time to recharge pressurised air. Some older lines still use manual braking when braking power is limited, as for the San Francisco cable cars [23].

In 1869, the Westinghouse air brake system (WAB) was patented [22], followed by an improved version in 1872. As opposed to the previous system which required direct air supply from the locomotive to activate, the WAB included an air reservoir on each wagon pressured to about 5 bars by the brake pipe when not braking, as well as a control valve. A reduction in air pressure in the brake pipe leads to brake application. This had two main benefits. The first was that it removed the necessity to pressurise the entire pneumatic system should brake application be required. The wagon air reservoirs are refilled after braking. Secondly, it was fail-safe as the brakes were automatically activated in case of a leak or wagon separation. The drawbacks were that the system was somewhat more complex (due to the air compressor requirements, as initially, these were quite complicated) than several competitors (chain brakes or simpler vacuum brakes). Moreover, releasing the brakes completely before reapplication was initially required, in essence removing brake power during this period as the air reservoir needed recharging. The braking performance was however superior as shown by e.g. the Newark trials in 1875 [22], where it was compared to other solutions available at the time (vacuum, hydraulic and chain brakes).

The system in use today is still very similar to WAB. Several examples of brake blocks used are shown in Figure 2.4. Brake actuators and air compressors have over time become more capable and efficient, and gradual braking capabilities have solved the issue of requiring full release before reapplication. The signal is however still carried by air pressure, limiting the signal velocity to the speed of sound in air, or approximately 343 m/s, although in practice substantially lower due to fluid resistance in the brake pipe. This leads to relatively slow application times for the longer trains. Some further developments have been proposed regarding the shortening of response times, for example implementing radio-controlled end-of-train devices so that the brake signal is sent from both ends of a train, and reliability improvements in the mechanical components. Using electric signals (wired or wireless) have been attempted, with electrically controlled pneumatic brakes being used in some countries and proposed as mandatory in the US, although criticism regarding the cost vs benefit of implementing the system has arisen [24]. More will be discussed regarding electrification in Chapter 9.

Current research topics are mainly related to noise emissions, rolling contact fatigue, maintenance, wear and thermal capacity of the wheel. Additionally, the current EU project on digital automatic couplers (DAC) [25] would require electrification of European freight wagons. This opens up the possibility of also having electrically controlled brake actuators on freight trains, either as electro-mechanical or electronically controlled pneumatic actuators. This would enable more or less instant brake control, possibly also individual brake control of each wagon or wheelset.

Figure 2.4: Brakes blocks used on different trains in different eras. From upper left, row by row: 1) Japanese C62 steam locomotive, 2) Japanese KuMoHa 40 passenger car, 3) EF81 electric locomotive used on 'Twilight Express' services in Japan, 4) Series 7000 tram used in Hakodate city, 5) SJ B10 passenger car in use on the Stockholm-Uppsala commuter line 6) Fammoorr type 050 freight wagon as used on the Swedish-Norwegian Iron ore line.

2.3 Wheels

The first body of concern in tread braking is the wheel. Wheel design has evolved over the years with increased knowledge and computational capacity. Modern tread braked wheels often have S-shaped webs designed to give a good trade-off between residual stress resistance and compliance, compared to older ones where the web is more straight. There are however a multitude of designs, and the effect of braking will then differ for various wheels. Primarily, it means that currently compliant wheels may fail during future scenarios not envisioned during the design. An overview of a wheel is shown in Figure 2.5.

Requirements on wheels of relevance to this work are given in European standards EN13262 [12] and EN13979 [11]. The latter covers geometry, thermomechanics, mechanics and acoustics whereas the former specifies characteristics for railway wheels, such as material specifications and requirements. Amongst other requirements, the initial residual stress (i.e. after forging) is required to be more than -80 MPa, as the compressive stress has a positive effect on the fatigue resistance. With regard to braking requirements for wheels using European steel grade ER7, EN13979–1 details both allowable residual stress (less than +200 MPa or +275 MPa average residual circumferential stress for new and worn wheels, respectively, although maintenance standards allow for higher values [26]) as well as allowable displacement (within +1,5 and -0,5 mm after testing). In this case, brake testing requires 10 cycles of 50 kW for 45 min at an average speed of 60 km/h for normally sized tread braked wheels (840–1000 mm diameter). Long-term drag braking is considerably more damaging with respect to thermomechanics than stop braking due to the significantly larger amounts of absorbed energy, and will therefore generally be the limiting case for global thermal damage on wheels.

The situation of overheated wheels is of significant structural concern. Due to the higher thermal conductivity of the steel material of the wheel compared to the composite or sintered block material (as cast iron is being phased out, see next section), the major part of the produced heat enters the wheel. During short-term stop braking sequences, the surface can generally reach several hundreds of degrees Celsius [27–29]. The short durations of the heat applications tend to preclude significant damage or residual stress accumulation beyond a region close to the surface, however. For prolonged drag braking situations, as described above, the wheel temperatures can reach 400 °C in normal service and 600 °C in extreme conditions. On wheels in lab testing,

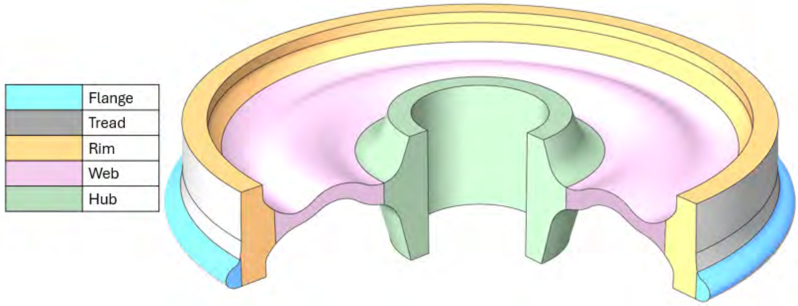

Figure 2.5: A model of a railway wheel with several parts pointed out.

hot spots above 900 °C have been observed, see **Paper C**, although the small size and rapid wear tend to limit the mechanical effects.

It should be noted that the extreme lab testing of temperatures is not just of theoretical concern. Railway wheels are exposed to significant mechanical loads during normal service, and the addition of severe heating reduces the steel strength and exacerbate damage. Several major incidents involving wheels broken or damaged through thermomechanical effects have been observed in Europe. In 2016, broken wheels of two types, BA314/ZDB29 and BA004, the latter of which has been used in some testing in **Paper D**, were investigated [30] and the cause was determined to be thermal overload or possibly thermal loading combined with rolling contact loads. A more detailed description of the processes involved is given in Chapter 4. These incidents have resulted in proposals for changed wheel utilisation and amendments to standards and regulations concerning the actual thermomechanical requirements of the wheel designs. Additionally, methods for detecting thermal overloads of wheels and regulations on braking to prevent such failures have also been proposed [30].

2.4 Brake blocks

The other main component in the braking system is the brake block, examples of which are shown in Figure 2.6. For modern brake blocks in Europe and elsewhere, the traditional cast iron brake blocks are being supplemented or replaced by composite organic or composite sinter brake block materials. The

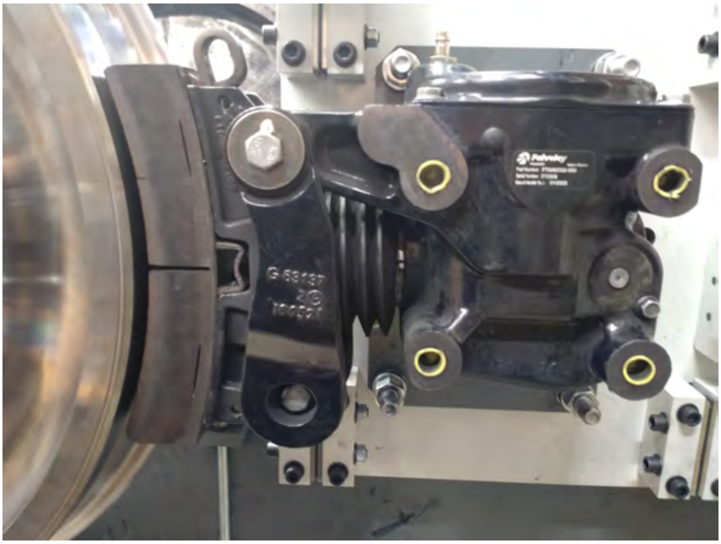

Figure 2.6: BFC unit in the Chalmers Brake Roller Rig, showing an example of how a tread braking unit is mounted.

main reason for this is the noise emissions that occur. In the 1990s, tread braked vehicles with cast iron brake blocks were found to generate higher noise levels compared to vehicles with disc brakes or ED brakes. Reduction of this rolling noise, related to the overall use of cast-iron brake blocks, has ever since been a significant challenge, with for example several previous projects at European level, in which CHARMEC has been a partner. This includes *EuroSABOT*, *Silent Freight* and *Euro Rolling Silently.* Braking using organic and sintered composite blocks generates significantly less rolling noise than wagons braked with cast iron blocks [31] due to lower wheel roughness, as the cast iron tends to deposit material onto the wheel surface, forming patterns that contribute to noise emissions. One outcome of these projects of particular relevance for this thesis is that the switch to composite materials leads to a larger amount of heat entering the wheel due to lower conductivity of these block materials compared to cast iron. In principle, this is where the work performed in the current thesis has its roots.

Overall, significant efforts have been made to decrease the noise emissions from railway traffic. The first European directive, 2001/16/EC [32], concerning the interoperability of the Trans-European conventional rail network, was enacted in 2001. This contained provisions for noise problems deriving from rolling stock and infrastructure. The directive was then updated in 2008, with technical specifications for interoperability to the rolling stock part of the high-speed rail system [33, 34]. Further amendments were then added in 2011 [35] and 2014 [36] so that it encompasses noise emissions of general rolling stock. Although not directly stated, the regulations implicitly ban cast iron brake blocks in the European Union (with some temporary exceptions for Sweden and Finland due to winter braking concerns) as cast iron blocks are overall unable to fulfil the rolling noise criteria.

The composite materials present an opportunity for tailor-made blocks for specific operations as the material properties can vary significantly depending on the constituents. The service life of composite brake blocks is generally longer than for cast iron brakes [37]. From a wheel point of view, the blocks should have high thermal conductivity so that more heat flows into the block. In [38], the heat partition was calibrated using experimental data, showing that cast iron blocks absorbed 13-24% of the total heat load whereas composite and sintered blocks only absorb 4-14% (higher absorption for sinter). Increased temperatures on the brake block increases wear rate [39–41], causing higher maintenance costs and particulate emissions. Nonetheless, modern non-cast iron blocks are designed to achieve low wear rates at normal operation, but very high wear at higher temperatures [41] to prevent dangerous situations when brakes are, for some reason, locked. Thus, the brake block should act as a thermal fuse in service [41], in essence requiring that the block wears away quickly above certain temperature levels to prevent excessive heating of the wheel. Severe damage or fracture to the wheel could lead to derailment, whereas a worn down brake block can relatively easily be replaced. The high wear of the brake block is however in itself problematic as emitted particles may serve as ignition sources of e.g. forest fires [42, 43].

There are also requirements on the friction coefficient of the material, which in turn will affect the braking process, primarily for composite blocks intended to be a replacement for cast iron blocks [41]. Furthermore, the friction coefficient is also temperature dependent, generally decreasing with increased temperature and pressure dependence, normally decreasing with increased pressure. This can be seen in Figure 2.7, which also indicates that the friction coefficient can vary between tests, although tested by manufacturers to be inside a specific range for homologated speeds. This showcases an issue in that it is difficult to control the actual braking power on the train, in particular with multiple wagons which may have differing braking capacities due to wear, slack adjustments, icing or other variables. Electrically controlled brake units may improve this, but are still years away from being widespread in freight service.

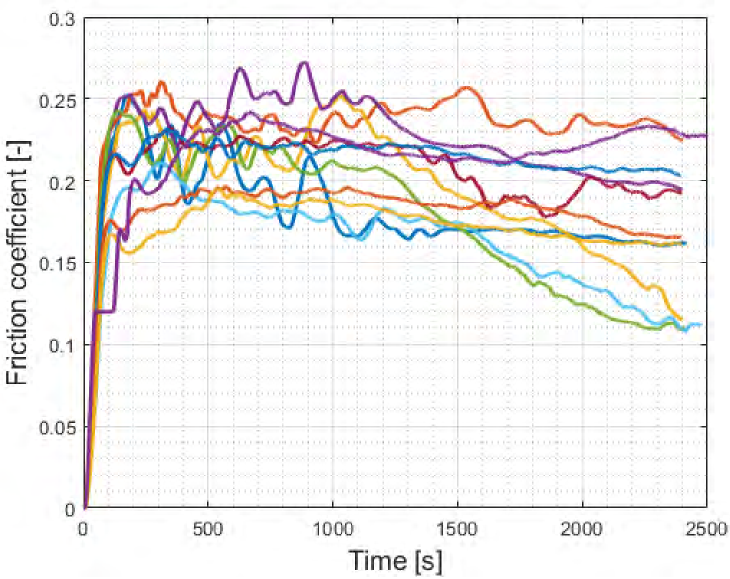

Figure 2.7: Friction coefficient through the drag braking process for several different tests, with the same test setup but at various braking powers.

CHAPTER 3

Frictionally induced effects and tread braking

The thermomechanics of braking is a complicated topic that has been extensively studied over many years. This chapter intends to concisely describe the thermal and thermoelastic phenomena that occur during the braking sequence, as well as some of the research that has been done on the topic. The mechanical aspects of the loading of the wheel is left out, since it is the subject Chapter 4. Generally, the complex interaction between the brake block/pads and the wheels/brake discs does not lend itself to being easily described. Although the problem can be considered axisymmetric with well-defined contact pressure, friction and generated heat flux as a first-order approximation, this description rapidly is found insufficient.

The first part of the chapter introduces the overall modelling methods and the mathematical assumptions that govern the heating and cooling processes. This is then continued with a description of the instability processes that occur in a frictional sliding contact system and how non-uniformities in the heat flux and thus, the temperature field, arise. Finally, it ends with a description of global non-uniformities, i.e. when the temperature field tends to form longer wavelength modes or combined wavelength modes, which has not been studied in depth elsewhere for tread braking systems.

3.1 Description of frictional braking

When the brake is applied to either the wheel (in the case of tread braking) or the brake disc (in the case of disc braking), heat is generated by converting the kinetic or potential energy of the train almost entirely into friction thermal energy via the frictional interface between the contact surfaces. An example is shown in Figure 3.1, where a glowing line can be seen on the wheel rolling surface. The generated heat flux q can at a basic level be approximated as

$$q = \mu p v \tag{3.1}$$

where μ is the coefficient of friction, A is the contact area, p is the normal pressure and v is the rolling speed of the train. This heat can then be partitioned between the two contacting bodies through various assumptions. One method of dividing the flux is through the concept of thermal resistances. This is derived in a previous work [10], based on an apparent temperature jump existing at the frictional interface. The heat flux into the wheel and brake block, respectively, can then be written as

$$q_w = \frac{T_b^{cont} - T_w^{cont}}{R_w + R_b} + \frac{R_b}{R_w + R_b} q \tag{3.2}$$

$$q_b = \frac{T_w^{cont} - T_b^{cont}}{R_w + R_b} + \frac{R_b}{R_w + R_b} q \tag{3.3}$$

Here, q_i is the heat flux, T^{cont} is the contact temperature and R_i is the thermal resistance pertaining to the body (with values for the studied contact pair) with the subscripts w and b denoting wheel and brake block parameter, respectively. q is the previously defined generated heat flux. Because of the difficulties in accurately modelling the complicated behaviour of pressure and friction, these are normally determined from experiments.

Additionally, cooling flux is introduced via both convection and radiation using the classical formulae

$$q^{conv} = -h^{conv}(T - T_{amb}) \tag{3.4}$$

$$q^{rad} = -\varepsilon\sigma(T^4 - T_{amb}^4) \tag{3.5}$$

where h^{conv} is a calculated convective coefficient as developed in [38], T_{amb} is the ambient temperature, ε is the emissivity of the surface and σ is the

Figure 3.1: Wheel during drag braking applications, where the high tread temperatures in the brake contact strip cause the steel to glow.

Stefan-Boltzmann constant. Analytical solutions for the heat partitioning between the wheel and brake block, as shown in [44], are also possible, with assumptions of e.g. 1D heat flow behaviour, rigid bodies, no material dependence on temperature and perfect contact.

The focus of the previous formulation was to determine the *average* temperature fields that arise during the braking process, rather than trying to model the instabilities that also occur. This modelling approach is not capable of producing spatially non-uniform fields, which means that a complementary description is required.

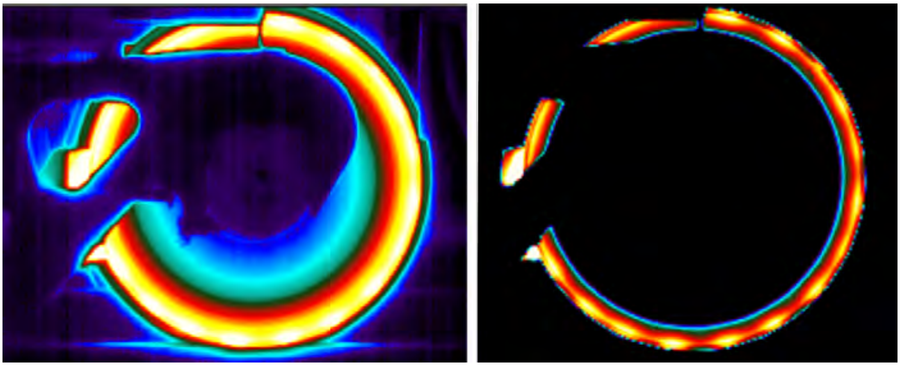

Figure 3.2: Thermographic images of the same tread braked railway wheel. By increasing the contrast in the left image, the hot spots (TEIs) become clearly visible on the right.

3.2 Thermoelastic instabilities

Two surfaces in sliding contact are never perfectly regular, and surface irregularities will inevitably result in some non-uniform contact pressure distribution. These distributions will then cause non-uniform heating. Indeed, it has been shown that even for smooth surfaces, the generated interfacial heat may cause irregular pressure distributions during sliding [45, 46]. This will lead to the phenomenon known as ThermoElastic Instabilities (TEI), wherein areas of the surface are heated in contact and, due to thermal expansion, locally expand. For sufficiently high speeds, the expansion increases local contact pressure and thus frictional heating, forming an unstable system where minor parts of the surface receive a significant part of the heat. This process is counteracted by e.g. wear and flexibility. Examples of TEIs are shown in Figures 3.2 and 3.3, where they are seen as hotter spots on the wheel rim and tread, respectively.

For railway brake blocks, the sliding surfaces were early studied for spoked wheels in [47] where it was found that contact was isolated to thin strips of the brake block. This led to energy dissipation over very small areas due to the interaction with the wheel tyre, with the result that the tread formed bulges that can be considered a type of thermoelastic instability. This was then reinforced in [48], where the formation of thermoelastic instabilities for the case of frictional sliding between two solids was studied. The experimental measurements confirmed the existence of the TEIs, with calculations showing that even almost perfect surfaces would exhibit these instabilities above some specific critical velocity. Closely thereafter, the formation of TEIs was studied analytically for the case of blades sliding along a thermally conductive body. It was noted that for the assumed temperature disturbance T, described by

$$T = T_0 e^{-by} e^{\sigma t} \sin \omega x \tag{3.6}$$

the exponent σ would be *positive*, i.e. amplifying any initial disturbance, for sliding speeds above a critical speed V_n for the studied perturbation wavelength. This critical speed was dependent on the coefficient of friction and conductivity. It was concluded that for the essentially stochastic sliding (i.e. how non-uniformities would contact) process, surface contact could change from uniform to non-uniform pressure and temperature distributions. In [49], an analytical solution for the sliding of thin tubes was found using the same postulated sinusoidal solution. For disc brakes, in [50] a solution was found when a pressure perturbation of the type

$$p(x,t) = p_0 e^{ct} \cos mx \tag{3.7}$$

with an associated non-uniform frictional heat flux was assumed. For block braking, no analytical solution has been found that shows this behaviour.

A numerical study of the TEI-problem was first made in [51], where it was shown that a thermoelastic analysis could predict instabilities, where after more sophisticated models have evolved demanding increased computational power. Further models have investigated the eigenvalue or modal solutions through various methods. Fourier reduction of temperature fields of the type $T(x, y, z, t) = e^{bt}\Theta(x, y, z)$ was studied in [52]. It was shown that although good correlation between numerical solutions and experimental results for axisymmetric problems could be gained, accurate characterisation of materials remained a difficulty. A non-modal problem is solved in [53], where migration of hot spots was also included, showing that even for multiple unstable modes the final state tended towards single dominating modes. An improved analysis was then made in [54], where a modal analysis of a multi-disc clutch or disc brake was performed, where the excitation of unstable modes could be seen. Additionally, it was shown that only perfect models for in-plane sliding would exhibit stability and that for all others (non-uniform in-plane or both uniform and non-uniform out-of-plane), instabilities would be excited. A 3D finite element model was used in [55], showing that neglecting the wear would not only lower critical speeds significantly but also not produce a periodic solution.

For block brakes, the contact problem was studied numerically in [56] using a 2D model which included Archard wear and an initial pressure distribution which included random disturbances. Herein it was shown that even for small disturbances, very fast growth of the perturbations was predicted. Quantitatively similar behaviour compared to experiments using both cast iron and composite blocks was seen, although it was noted that the limitations of the 2D model prevented occurrence of some expected behaviour.

Regarding wear, its effect has been detailed in several studies [57, 58]. In these, it can be noted that although wear is usually positive with regard to removing the thermoelastic instabilities, there are cases where it destabilises the process [58]. For the tread braking system, the wear between the wheel and brake is not necessarily large enough to remove the hot spots, as evident in [28] where the hot spots are shown to be almost entirely stationary in some cases.

The experimental study of the phenomenon of thermoelastic instabilities was initially hindered by insufficient measurement methods [48, 59]. Single drilled-in rotor-mounted thermocouples are unable to resolve the surface variations because they are stationary with respect to the rotating wheel, and ordinary sliding thermocouples suffer from large time constants. Radiometric methods, in particular high-speed optics, alleviate the thermocouple issue in that the surface can be imaged at several hundreds or thousands of times per second. This is, however, not a true panacea as the surface emissivity is not well-defined due to surface oxidation at higher temperatures, but overall patterns are evident. Additionally, it is not possible to directly observe the actual wheel and brake block surfaces when they are in contact. Partially, this is because opaque objects obstruct the view and the high pressure can damage any contact probes. For rotor surfaces outside the contact patch, auxiliary train-mounted equipment pose observation problems, in addition to issues related to mounting high-grade optics to the undercarriage of a train wagon. It is, however, possible to observe rotor surfaces in lab conditions using high speed radiometric methods (kHz frame rate measurements), or by using low-cost bolometer (frame rates typically in the range of hundreds of Hz) type equipment under wagons [60].

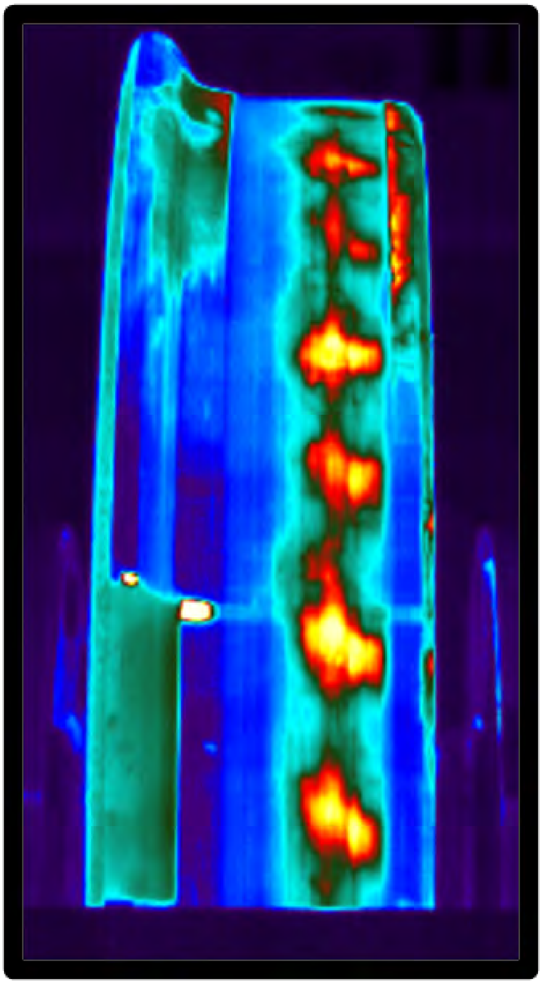

Figure 3.3: Image of thermoelastic instabilities on the wheel tread. The bright hot spots can be seen in red and yellow, contrasting with the colder surfaces in blue and green. Note that the small bright spot is a reflection of a ceiling lamp, indicating one of the difficulties of performing radiometric measurements.

An additional issue is that the behaviour of hot spotting varies significantly depending on brake materials and braking parameters. In [61] six different types of TEIs are given, and the dominant type varies with e.g. speed, brake pressure and friction material. Although intended as a study for automotive systems, the general behaviour is similar for railways based on experimental experience reported in [27].

As noted in the preceding paragraphs, there are models capable of determining the instability conditions and the resulting modes for disc braking scenarios [62, 63]. Several of these models are capable of computing critical speeds above which stable (uniform) solutions are inadmissible, as well as maximum hot spot temperatures, Wear levels where instabilities are reigned in are also results shown. It should be noted however that actual comparisons of measurements and numerical predictions are few [64–66].

For block braking, there are no accurate global models of the phenomenon, as the transient contact on the wheel tread is somewhat more complicated to describe and axisymmetry no longer applies. General numerical methods are still applicable, but solving e.g. fully coupled thermomechanical problems tend to be computationally difficult, especially if the aim would be to capture maximum temperature at hot spots, which would be the case regarding the present work. Such models would potentially include non-uniform surfaces (on both contacting bodies), wheel rotation (and thus intermittent contact), material expansion and material non-linearities, wear, third body modelling [67], non-linear cooling (convection and radiation) among others.

A different approach is to focus on the surface temperature field that is known from experimental results presented in the present and other works, and suitably fit surface thermal fluxes based on analytical functions, to mimic observed temperatures. By using the a priori calculated temperatures in the mechanical analysis and then sequentially coupling (i.e. ignore the mechanical effect on the temperature field) them, the thermal effects on the mechanical state can be computed. Solutions that account for non-uniform temperatures without significantly increasing computational complexity are then possible, although the local effects that occur in or close to the actual contact between wheel and brake are disregarded. This method is utilised in **Paper C** and **Paper E** to determine the effects on the wheel caused by the non-uniform heating.

3.3 Thermal localisation

Another issue not well studied hitherto is the phenomenon of Thermal Localisation (TL), in essence, that the heat flux is not evenly distributed over the wheel circumference, giving rise to a global non-uniform temperature field [28, 29, 68]. An example of this is shown in Figure 3.4, where the left wheel is almost evenly heated during braking and the right wheel shows a significant difference in temperature between the left and right halves. Field measurements on trains in field conditions in Australia [68] and on the Norwegian Ofotbanen [29] have shown that this phenomenon is relevant for revenue traffic, but only on a few wheels even during scenarios with relatively high thermal loads. On the other hand, at brake rig testing, these phenomena has occurred for every wheel tested at Chalmers as well as the one used at RTRI for stop braking tests.

The TL contrasts with TEIs, which are significantly smaller and show higher peak temperatures due to the more concentrated heat flux. TLs also causes other issues to arise. Thermoelastic instabilities, although in some studies noted to be quasi-stationary [28], can be suppressed by rotor wear [57]. The larger non-uniformities do not necessarily present the same possibility to be suppressed, simply due to the significant volume of wheel material. The TL also presents another issue, as it has been shown [28] that increasing the heated volume significantly affects the residual stress field. This in turn is expected to increase the likelihood of thermal cracks [69].

Unlike the thermoelastic instabilities which can be explained with unstable modes as noted in the previous section, where the dominating wavelength often can be related to the contact length of the friction material, no such analysis results in a first-order mode appearing. It is evident that some form of initial or induced (i.e. during the braking sequence) out-of-roundness results in uneven brake contact pressures for part of the wheel tread, which then amplifies the thermal flux and leads to TL. From the available data, the phenomenon seems to be related to the magnitude of the heating of the wheels, in that hotter wheels show significantly higher incidence rates.

One hypothesis for the phenomenon has been manufacturing defects causing out-of-roundness from the heating during the braking process [68]. In essence, the wheel is inherently out-of-round, but this is then presumed to manifest itself only during heat application, causing an uneven contact pressure with resulting uneven heat flux as described in the above paragraph. A second hypothesis for influencing factors has been the stiffness and hysteresis of the brake actuator. Brake riggings on trains in service are generally more compliant than mountings in brake dynamometers. Any existing out-of-roundness would then be elevated as the brake actuator does not adjust well to the variations in radii, despite the pneumatic actuator and its inherent flexibility, causing a varying brake normal force and uneven contact pressure which results in uneven heating. This is despite that the brake block itself tends to be relatively compliant with low Young's modulus [70]. The system seems to act more as a displacement-controlled one rather than a force-controlled system. This latter hypothesis is supported by the fact that the incidence rate is higher in brake rigs, although the number of tested wheels is low.

A related problem is the detection of non-uniformly heated wheels in revenue service. Detection of these non-uniform phenomena is difficult, as trackside detectors generally measure either single point temperatures. Thus, they do not give enough information to determine circumferential temperature variations, or flange areas, which tend to mute temperatures due to the larger volume of material and conduction distances [71].

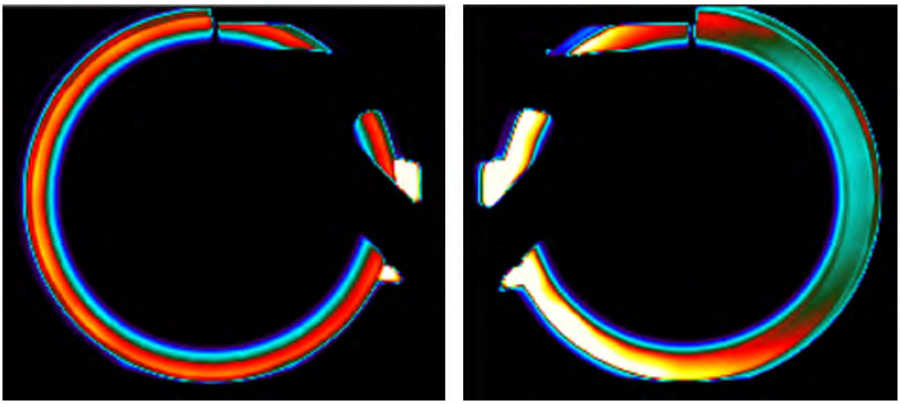

Figure 3.4: Thermographic images of two different tread braked railway wheels illustrating thermal localisation. The left wheel is nominally evenly heated, whereas the right wheel shows an approximate 50 °C difference between the left and right halves.

CHAPTER 4

Thermomechanics of tread braking

The process of braking is inherently thermomechanical. As the brake is applied, frictional heating introduces elevated temperatures which induces strains and stresses whilst the wheel is rolling with the rail. This leads to a phenomenon where the thermomechanically induced loading and the mechanical loads interact, often leading to plastic material response as well as wear of the bodies.

This chapter begins with the thermomechanical problem, wherein the thermal loads induce a temperature gradient in the wheel with a hotter tread and rim, and a colder web and hub. This may cause compressive yielding of the wheel steel if the gradient is significant enough, resulting in tensile residual circumferential stress after cooling, which can promote fatigue and fracture. Finally, descriptions of effects of wear and wheel thermal damage are given in the final two sections.

4.1 Thermomechanical loads

In the previous chapter, it was shown how the wheel heats up during the braking sequence. From basic solid mechanics, one knows that the thermal expansion of a material can be written as $\varepsilon_{thermal} = \alpha\Delta T$, where $\alpha = \alpha(T)$ is a temperature-dependent coefficient of thermal expansion and ΔT is the temperature difference compared to some initial temperature. Uniform heating without constraints would then lead to stress-free expansion. With the temperature gradient that forms during the braking, the thermal expansion varies over the entire wheel, constraining the hotter material which leads to to stresses. The gradient can be quite large at significant heating, as shown in Figure 4.1 which details the calculated temperature and stress fields during one braking sequence at different times for $P_{brake} = 50$ kW for 45 min, as laid out in the wheel design standards [11]. In Figure 4.1c it can be seen that the stress field is compressive. Although the values are relatively low, it should be considered that the yield limit at 600 °C is approximately 50 MPa [72]. The wheel begins to yield in compression at about 900 s for this specific case, which induces a significant amount of plastic strain during the latter two-thirds of the braking cycle. The procedure is in a sense reversed as the wheel then cools down, see Figures 4.1e and 4.1f. The induced plastic strains will then cause *tensile* residual stresses in the wheel rim, primarily acting in the circumferential direction.

The EN 13979 [11] standard details limits for the average residual stress as measured in the wheel rim. For new wheels with a diameter of 920 m, the stress should remain below 200 MPa whereas the wear limit for a worn wheel at 840 mm is 275 MPa. These values are specific to ER7 steel wheels. An ultrasonic method determines the average stress over a small volume thanks to the probe design [73]. It works by measuring the time response of the reflection of an ultrasonic wave, which is dependent on the stress field in a material. Results from such measurements show lower values of average stresses towards the hub and higher values towards the tread. The detailed stress field is difficult to determine, in principle requiring destructive testing [12]. Other methods are also limited, with X-ray measurements being restricted to surface stresses. Additionally, measurements may be sensitive to non-uniform heating, increasing the residual stress levels locally. Example results of average residual stress measurements in **Paper D** is shown in Figure 4.2. Here, the residual stress field has been measured at 12 circumferentially evenly distributed points

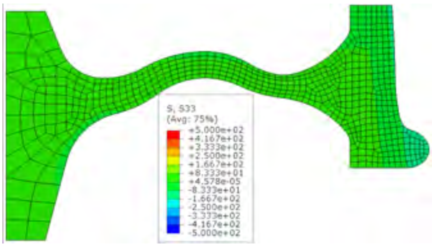

(a) Stress, t = 0 [min]

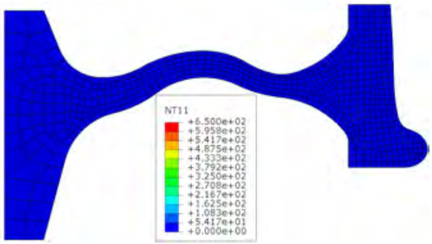

(b) Temperature, t = 0 [min]

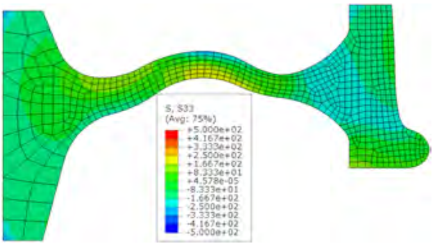

(c) Stress, t = 45 [min]

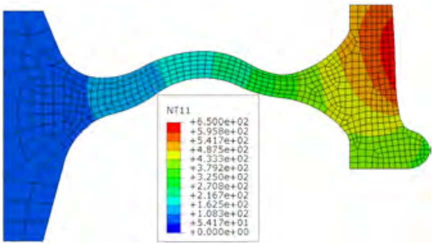

(d) Temperature, t = 45 [min]

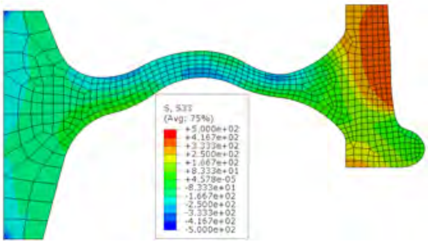

(e) Stress, t = 45 [min]

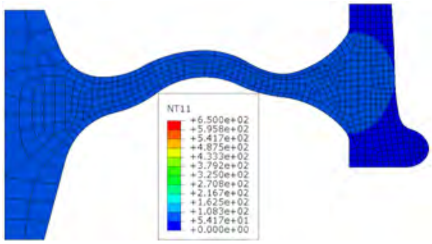

(f) Temperature, t = 45 [min]

Figure 4.1: Calculated circumferential stresses (left) and temperature fields (right) in the wheel cross-section during a 45 min, 50 kW braking cycle at three time instants, showcasing how the material yields during heating. Note that as the temperature increases, the material itself becomes weaker, leading to low stress values at 45 min.

on the wheel rim (field side) after 11 different braking cycles.

The primary issue with high tensile residual stresses is that it can lead to, in the presence of some stress concentration (primarily small cracks), fracture of the wheel upon cooling. This would then result in a radial crack that either extends to the hub or branches back to the tread. The former would induce global wheel failure and cause significant damage, likely derailment, should the wheel be used for continued service. The latter may cause spalling of small or large chunks of material should it occur, leading to track damage.

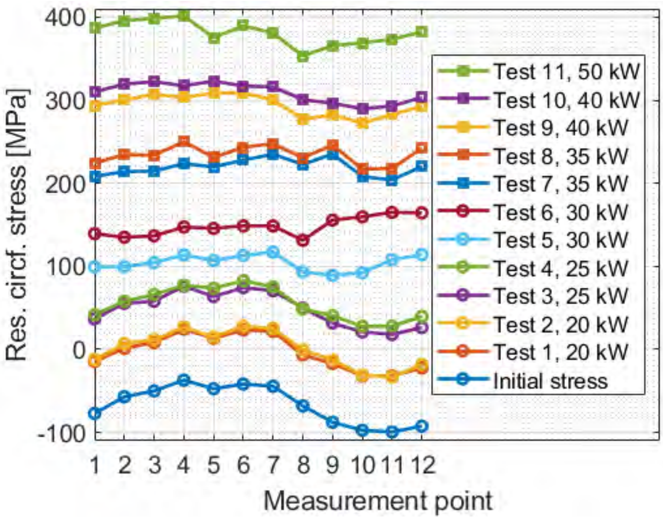

Figure 4.2: Residual stress field evolution at 12 equally spaced points around the wheel circumference, for 11 drag braking tests each at the indicated power level.

4.2 Fatigue and fracture of railway wheels

Fatigue is the initiation and propagation of cracks in materials due to cyclic loading. The cracks, once initiated, can grow during the loading cycles until complete structural failure occurs. For railway wheels, cyclic loading primarily refers to the variation in mechanical loads experienced during rolling, due to the periodic contact loads resulting from the wheel-rail contact. An example is given in Figure 4.3 where the contact patch on which a force of fifteen tonnes is concentrated on, as well as the resulting plastic deformation. The generated contact stresses are some of the largest in engineering applications [74]. This is referred to as Rolling Contact Fatigue (RCF), where the wheel is rolling on the rail and the contact zone traverses around the wheel, with cracks initiating either in or below the contact (wheel tread) surface. However, despite the harsh loads, accidents are rarely caused by wheel fracture caused by RCF [75]. However, RCF is still one of the major issues that occur for the wheel component, being a substantial cost-driver, and has for this reason been widely studied.

Surface-initiated rolling contact fatigue is the more common but less severe type of RCF [75], with some low level of RCF on the surface likely being optimal as it shows that the system is being used to near to its capacity. The cause of this type of fatigue is the frictional loads between the contact surfaces, where the frictional stress causes stresses exceeding the yield limit in shear and thus plastic deformation occurs. Should this plastic strain exceed the fracture strain, surface cracks form [75]. The crack initially grows at a shallow angle [76], followed by almost radial growth thereafter. Finally, it usually deviates back to the surface, with a piece of the surface breaking off. Surface-initiated RCF is addressed through re-profiling, wherein the outermost material of the wheel rim is machined away until cracks have been removed, and a nominal profile is achieved. This process is however costly and requires taking the train out of service and removal of the wheelset depending on available maintenance facilities. Examples of this type of RCF are shown in Figure 4.4.

Subsurface-initiated rolling contact fatigue is more problematic. Failures due to this mode are rare, but the consequences are often worse. Significant damage to rail and bogie is a likely result, with a potential for derailment [75]. This type of fatigue is also more difficult to reveal since it occurs in the bulk of the material and not on the surface, requiring ultrasonic inspections, with minimum requirements on crack size [75]. The cracks are initiated through a

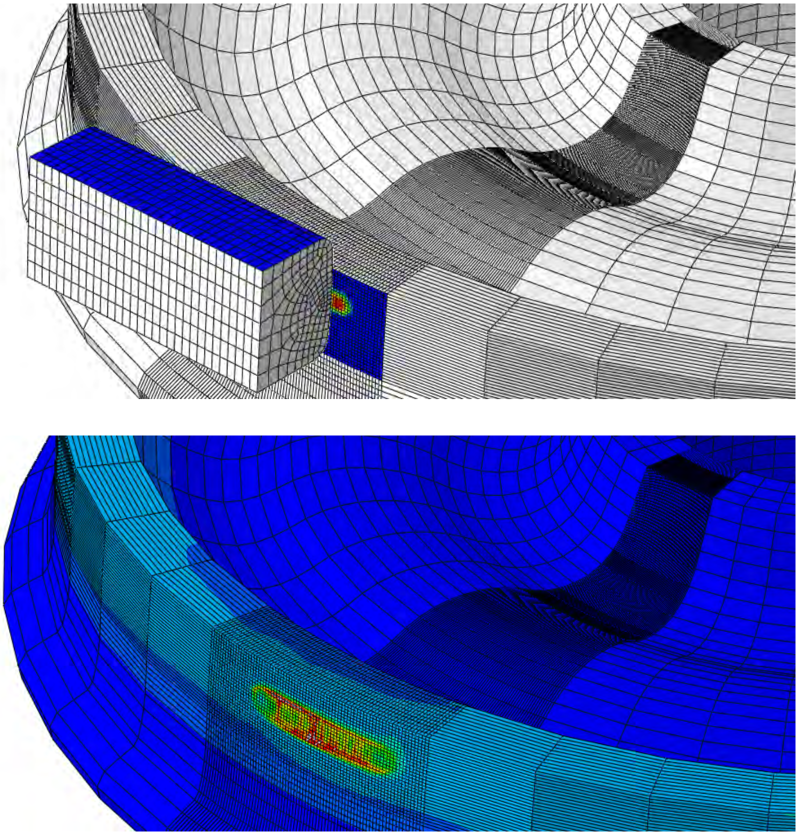

Figure 4.3: Above: modelled contact interaction between a wheel and a rail, indicating the contact patch. Below: plastic strain on the rolling surface after several rolling contact cycles.

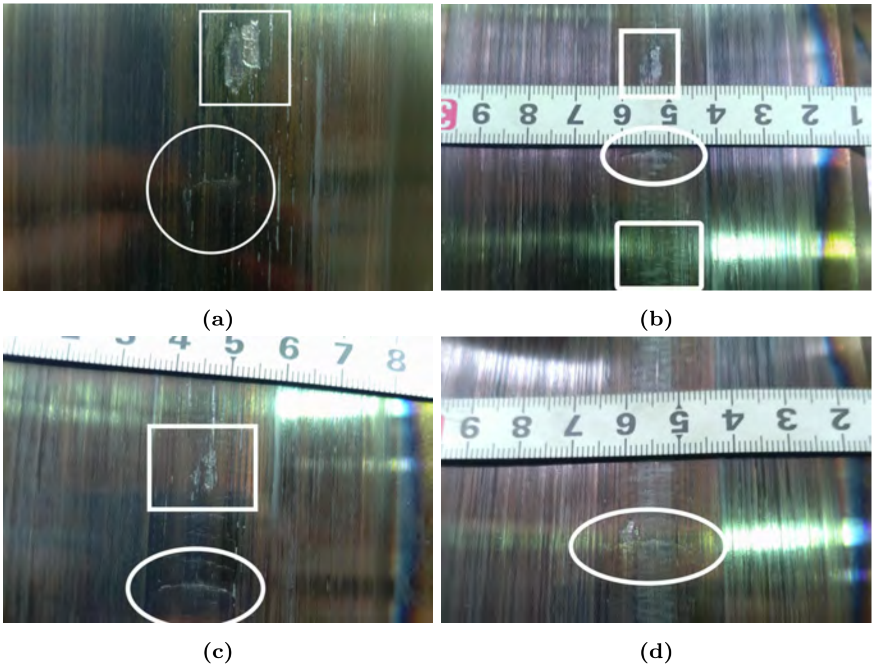

Figure 4.4: Crack evolution on the wheel rolling surface after a) 36 brake applications, b) 62 brake applications, c) 82 brake applications, d) 112 brake applications. The large noted crack is likely due to some crushing damage, whereas the faint lines are rolling contact fatigue cracks. The boxed or circled marks indicate the same crack or indentation in each image.

combination of the contact loads (which under Hertzian conditions have the largest shear stresses occurring some millimetres below the surface), material microstructure, residual stresses (from e.g. braking), contact geometry and material defects [75]. One reason subsurface-initiated RCF tend to be more critical than surface-initiated RCF is because of the type of failure, in that it branches either towards the wheel rim hub, with significantly larger crack sizes as a result.

Thermal loading due to the friction braking may cause a tensile residual circumferential stress field upon cooling down, which could initiate cracking in the wheel surface [75], resulting in very shallow cracks in mild cases. One could also note elevated temperatures on locomotive wheels may occur in high slip cases, although tensile residual stresses may not be the end result.

Previous research [69, 77] has concluded that purely thermal loads do not necessarily cause crack initiation in and of itself. Some form of tractive contact is required for this. In addition, the brake material may also affect the crack growth [19]. The same absence of crack initiation for cases without rolling contact has been observed in the experiments performed in the appended works in this thesis. Wheels with residual stresses even significantly above the UIC limits have shown no observable RCF. It should be noted that no comprehensive study regarding the total failure of a wheel has been performed in this work.

The main issue may instead be the interaction between thermal fatigue and mechanical fatigue [75]. Thermal cracks may continue to propagate during mechanical loading, and the propagation of mechanical cracks will be assisted by thermal loading. Simulations of scenarios including a pre-existing crack [78] have identified that severe braking scenarios may cause deep cracks, although only the worst cycles induce crack growth. Others [79] have observed that the phase transformations that occur in the surface due to thermal overloads result in martensite, which promotes RCF initiation due to the brittle nature of this steel phase.

4.3 Wear

Wear is the damage, gradual removal or deformation of solid material, for railways usually due to contacting surfaces. It is important for the mechanical components of railway systems as the removal of material is one of the main cost drivers. For brakes, it is generally defined as the material loss through the contact interaction between the wheel and the brake block. The brake blocks are considered to be a consumable item, given the significantly softer material and relative ease of changing worn-out blocks. They do however cause particle emissions as brake dust spreads from the block, which may have negative effects on human health. This is not studied in this work.

For the wheel tread surface, the wear is caused by the sliding contact interaction with the rail and the sliding contact between the wheel and brake block. Such wear can be significant even for standard service loads if temperatures are elevated, in the order of tenths of millimetres, after 30 to 40 repeated brake applications [80]. If the wheel is hot for longer periods of time, the wear is even further increased [81]. The wear itself can be due to multiple different factors [82], including plastification causing material displacement, spalling of wheel surface material and more. Figure 4.5 shows two examples of worn wheels, the first of which shows hollow wear compared to the nominal surface shape. The second one shows significant material displacement towards the field side of the wheel, in addition to material being ripped from the tread.

The normal issue caused by wear is the change in wheel tread shape. The rolling surface has a conical shape to provide curve steering and running stability, which is important both for safety and comfort. This change in shape will then affect the interaction between the wheel and rail, which may have negative effects on both the ride experience and the forces between the wheel and the rail, increasing damage on both components [83]. Although not used in the included works in the present thesis, the wear rate is generally assessed as

$$\dot{w} = k_w \mu p v \tag{4.1}$$

where k_w is a wear coefficient (that may depend on material hardness and temperature) [84], p is the contact pressure, μ is the coefficient of friction and v is the sliding velocity [85]. This equation illustrates the temperature and contact dependence of the wear, as the resistance weakens at high temperatures and the contact pressure for railway wheels is extremely high. This ties in with the overall performance in this project and the immediately preceding project [85]. It should be noted that there is a potential for a "magic wear rate" [86] which would remove induced surface cracks or remove asperities causing thermoelastic instabilities, but this wear rate would be difficult to achieve in practice.

Overall, the wear of the wheel and brakes is an important cost driver. Worn brakes can be adjusted to a degree, but will need to be replaced at some point. For the wheels, elevated or unexpected levels of wear may require shorter maintenance intervals or even special inspections and replacements, which can cause high costs as the train is taken out of service.

Figure 4.5: (Above) Hollow wear on a railway wheel, showing the difference at both tread and flange compared to nominal profile. Picture courtesy of Henrik Nordin, Lucchini Sweden. (Below) Thermal overload causing (significant) plastic deformation and material flow on a railway wheel.

Table 4.1: Chemical composition of railway wheel material ER7 (wt%, upper limits)

C	Si	Mn	Mo*	Cr *	Ni*	S	P	V	Cu	Fe	*Mo+Cr+Ni
0.52	0.4	0.8	0.08	0.3	0.3	0.015	0.02	0.06	0.3	Bal	0.5

4.4 Thermal damage to the material

Monobloc railway wheels are predominately made of different low or medium carbon steels [12, 87]. The European ER7-type of wheel steel is a medium carbon steel alloyed as detailed in Table 4.1 according to the specifications in [12]. During manufacturing, the wheels are rim-chilled [87] to achieve a fine lamellar pearlitic microstructure in the rim, turning it into ER7 steel. This increases the hardness and wear resistance. A hardness map of the wheel cross-section is shown in Figure 4.6, where it can be seen that the tread is 30–50 HV harder than the interior of the rim and more than 70 HV higher than the wheel web. The rim-chilling also induces *compressive* residual stresses in the wheel rim, which protects against fracture.

At temperatures in excess of 450 °C [72, 88, 89], the structure of lamellar pearlite deteriorates into a spheroidised structure, through a process called "spheroidisation". The spheroidisation rate is faster at higher temperatures, acting very quickly at temperatures above 600 °C. Essentially, this removes the hard and wear-resistant microstructure achieved through the manufacturing process which promotes increased wear [72, 84] and additional ratcheting damage through lowered material yield limits. Unlike surface cracks or hollow wear, this damage cannot generally be presumed to be perfectly undone by turning of the wheel, as it is impossible to separate the damaged material from the undamaged one. One benefit of the rolling contact is, however, that this will induce some additional plastic hardening through work hardening of the material near the tread.

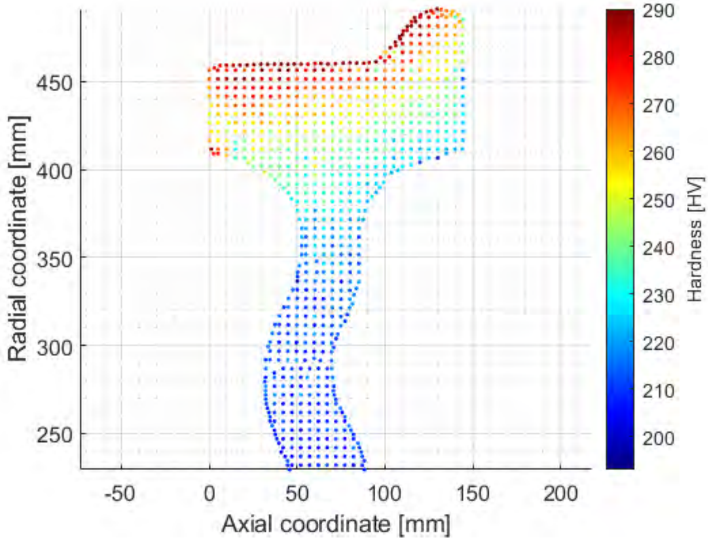

Figure 4.6: Hardness map of the wheel cross-section, showing the radial gradient.

CHAPTER 5

Modelling

One of the primary objectives of this work it to, through the usage of numerical simulations, gather knowledge on the limits of the tread braking system. By calibrating and further developing current models, better decisions can be made based on the numerical results. The primary method of knowledge building has been numerical simulations of tread braking, for both purely thermal and for thermomechanical scenarios. The finite element method (FEM) as implemented in the commercial software ABAQUS is used for the braking simulations, with most of the models described in this chapter being implemented as Fortran subroutines. The models used are based upon those developed in the course of several previous projects [10, 19, 38, 90–96], with varying degrees of changes introduced to adapt to the results from the work performed in the present thesis.

Section 5.1 of the present chapter introduces the thermal models used throughout the work in, before continuing with the material models in Section 5.2. Finally, an overview over possible future improvements is given in Section 5.3.

5.1 Thermal modelling

The first part of the thermomechanical modelling is, as can be suspected, the thermal one. As seen in Chapter 3, the thermal phenomena that arise are complex and difficult to describe. Several aspects should be considered:

- The heat initiates in the friction interface between the two sliding surfaces, in this case the wheel and the block. This turns it into a coupled thermal-mechanical problem.
- Nonlinear cooling, with both radiative, convective and conductive contributions.
- The boundary conditions are difficult to determine, as no surfaces are held at constant temperature.

As noted in Equation (3.6) from [48], an approximate solution of the thermal field is given from experimental observations, but no values are given for the parameters in the model. Initial attempts of modelling the heating were performed in the 1930s and 1940s [97, 98] and 1950s [99–101], by assumptions of equal contact temperatures. The interaction between the surfaces is however complex, with a "third-body" [67] arising. The heat is then generated in this interfacial body and then partitioned between the other bodies, in this case the wheel and the block, via thermal resistances as discussed in Chapter 3. Modelling based upon this is presented in [10, 38, 90] and forms a basis for several of the simulations performed in this work, primarily **Paper A** (as initial basis for the experiments) and **Paper B**. This approach is, however, designed for uniform heating. Non-uniform temperatures in disc brakes can be modelled via e.g. modal approaches [53, 54] due to the more symmetric loading case. For tread braking, approaches would require some form of uneven contact, as presented in [102]. This approach, which may result in the correct type of temperature field, also transforms the problem from a pure thermal simulation to a coupled thermomechanical one. To the author's knowledge, no such work have been attempted due to the difficulties involved.

For the work in this thesis beyond **Paper A** and **Paper B**, a Fourier series-type, exemplified in Equation (5.1)

$$q(\mathbf{X}, t) = \sin\gamma \sum_{k=0}^{m-1} \left[\frac{a_k}{A} \sin(\beta k) + \frac{b_k}{A} \cos(\beta k) \right]. \tag{5.1}$$

is used to describe the input heat into the wheel, and thus indirectly the temperature field. This assumption is based upon a frequency study of the non-uniform tread temperature field in **Paper C** and **Paper D**. For **Paper C**, only a qualitative study is made assuming stationary tread heat flux, and no calibration is performed. In **Paper E**, a study is performed on the modal behaviour of the temperature field, see Figures 5.1a and 5.1b for the time and frequency behaviour. This is then implemented numerically by a Fourier series assumption with time varying coefficients, calibrated based upon the experimental data. An example of a reconstructed field is shown in Figure 5.1c. There are several benefits of this, predominately the fact that the thermal solution can be computed in isolation and then sequentially coupled to the mechanical simulation, which improves computational efficiency. The accuracy of the solution suffers somewhat due to the approximation, but the overall mechanical damage studied is not affected significantly by the surface effects, as the stressed volume is small.

Cooling is introduced as a combination of surface radiation and surface convection, the latter as a custom subroutine originally derived in [10]. The convection is based on a cooling model for a rotating disc and accounts for, amongst other variables, radial variation in temperatures and rotational speed. Radiative cooling is introduced via the built-in routines of the finite element software.

5.2 Material modelling

As previously described, the wheel is exposed to a complex loading situation which combines substantially elevated temperatures, material damage, thermomechanical loading, thermoelastic interactions and significant rolling contact loads. Numerical modelling of the process provides an attractive option for the prediction of the wheel performance at braking. This modelling can be performed in several ways, depending on scope and required results. The finite element method (FEM) is the standard choice used in numerical simulations. Still, complex simulations such as rolling contact between wheel and rail for extended periods tend to require massive computational resources. This renders simulations time-consuming, often requiring restrictions on the size, interpolation, modal reductions or other solutions [19, 103].

Multibody simulations provide an alternative that can simulate the rolling

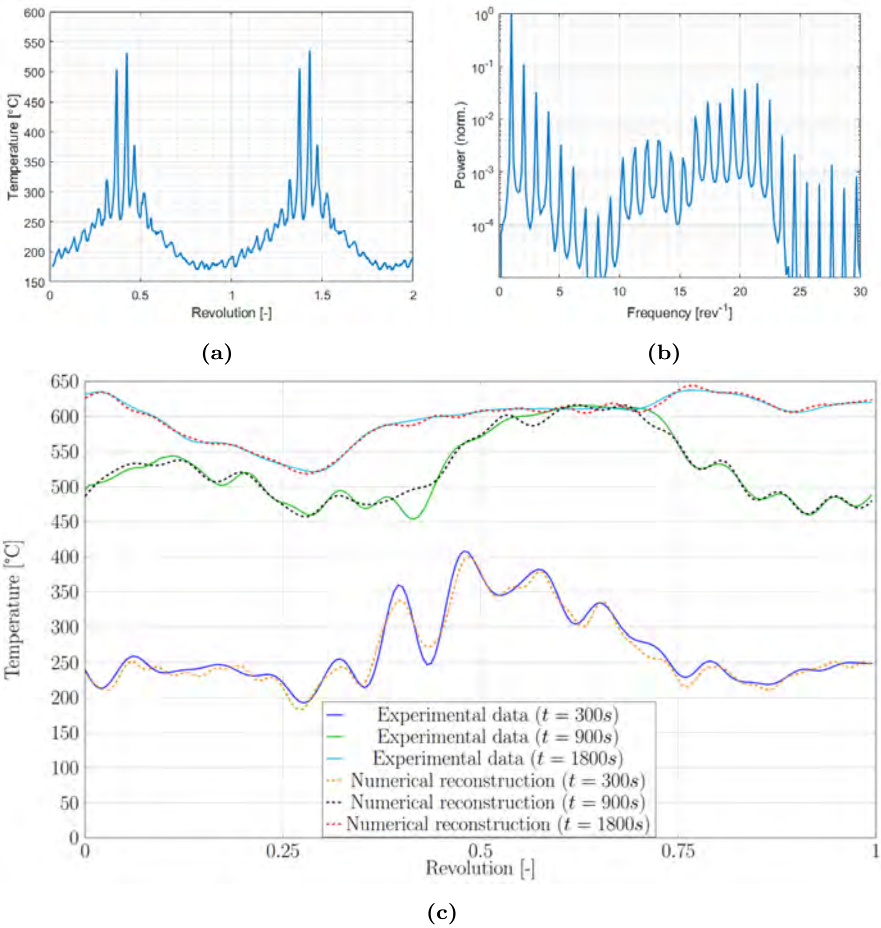

Figure 5.1: Illustration of the non-uniform temperature field at the centre of the wheel tread. a) Temperature field over the wheel tread for 4 revolutions, b) profile of power intensity per frequency and c) comparison of measured and reconstructed numerical temperature profiles.

process over larger geometries and periods [104] using rigid or elastic bodies combined with accurate approximations of the contact behaviour. Because of the loading situation of the railway wheels, there is a strong need to determine plastic response and material damage, and for this reason, this type of simulation is not an option. This is because material damage tends to drive costs. Cracks occur when the fracture toughness is exceeded, promoted by tensile residual stress fields which arise from plastic effects. Rolling contact can also initiate cracks on the rolling surface, or wear away material. These require detailed models to correctly predict and prevent.

The specific formulation used accounts for, as described in further detail in the coming sections, the below-listed phenomena.

- Nonlinear isotropic and kinematic hardening due to the accumulated plastic strains.
- Viscoplasticity (strain rate effects) due to the high loading rates during rolling contact, in particular at the elevated temperatures encountered during braking.
- Static relaxation of back stresses (i.e. stresses which shift the centre of the stress space), as can be seen from e.g. periods with constant strain during testing and possibly during long-term braking.
- Hardness corrections to yield and plastic behaviour as there is a gradient through the cross-section due to the rim-chilling treatment.
- Temperature-dependent material deterioration.

Examples of some of the above-listed material effects are shown in Figure 5.2.

The basis for the material model used in this thesis is the unified constitutive model as initially developed by J.L. Chaboche [105, 106]. This model is normally referred to as the Chaboche viscoplasticity model, shortened to the Chaboche model in the remainder of the text.

Limitations

The material models used are considered macroscale in that a detailed description of the microstructural phenomena is eschewed in favour of an amalgamated approach. Additionally, phase changes in the material which may

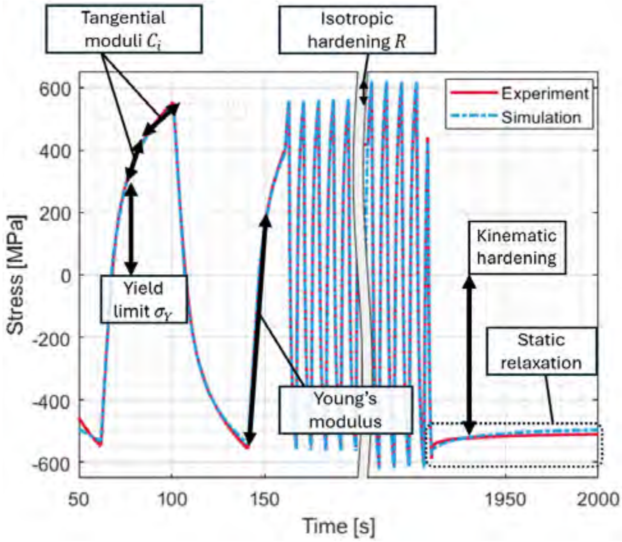

(a)

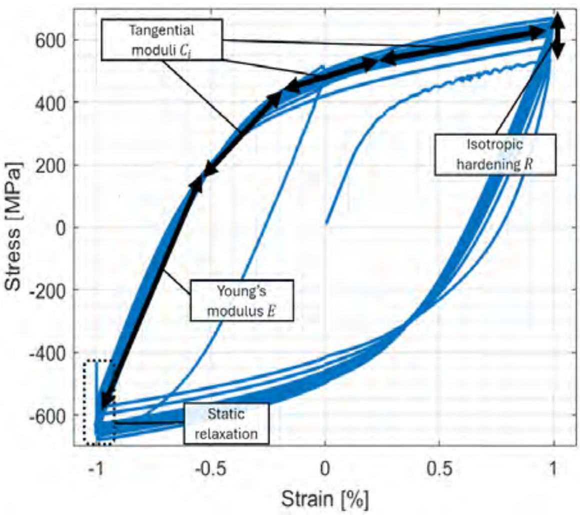

(b)

Figure 5.2: Material behaviour during isothermal strain-controlled tests, illustrating some of the material parameters for a a) stress-time curve, b) stress-strain curve.

occur at elevated temperatures are not accounted for. Instead, a simpler differential equation is used in this work to account for material deterioration by mimicking spheroidisation of cementite in the pearlitic steel.

The brake block-wheel interaction is fundamentally a coupled thermomechanical analysis, with the contact condition between the wheel and the brake block affecting both how the thermal energy is generated and how it is partitioned. Because of the complexity of this interaction, a sequentially coupled approach is used in which a thermal problem with presumed heat generation is used as input to the mechanical simulations. The thermal simulation is based on experimentally observed temperatures as noted in the previous section. The analysis does not account for the rapid heat pulses that act on the shallow zone near the surface during contact between the wheel and the other bodies, but only accounts for average effects of these contacts.

For the rolling simulations, not all revolutions are accounted for due to the computational requirements of the simulations. Instead, only a set number of simulations are performed, if possible, chosen so that the residual stresses and plastic strains in the surface tend towards a steady state.

Review of some other material models

The wheel material behaviour has been studied for several decades at this point. Initial models used have been either elastic [107] or elasto-plastic, based on available computational power and requirements. Some examples of elasto-plastic models used are given in e.g. [108–113], which includes the standard UIC thermomechanical model that was calibrated to reasonably fit results from brake rig tests using a linear kinematic hardening model.

These models are generally not capable of distinguishing the detailed behaviour of the highly loaded wheel steel and generally assume too high yield limits with low tangential moduli after yielding. However, for specific usage, they have found their place in research due to the ease of implementation, relatively short computational times and for the purpose an adequate accuracy. This behaviour can then be improved through the usage of one or more kinematic back stresses as first outlined in [114] and further developed in e.g. [105] where multiple non-linearly hardening behaviours are superimposed. With respect to the railway field, work using this type of model for studying freight wheels has been done over several decades [94, 95, 115]. Similar models, although not necessarily based upon the same framework, have also been used for rail applications in e.g. [116].

Model Description

A description of the Chaboche model, as implemented and used in the work performed in this thesis, is given in the remaining parts of this section.

The initial idea is to decompose the total strain into several independent parts, namely *elastic*, *plastic* and *thermal* strains, as

$$\boldsymbol{\varepsilon}^{\mathrm{tot}} = \boldsymbol{\varepsilon}^{\mathrm{e}} + \boldsymbol{\varepsilon}^{\mathrm{p}} + \boldsymbol{\varepsilon}^{\mathrm{th}} \tag{5.2}$$

The latter term is calculated as $\boldsymbol{\varepsilon}^{\mathrm{th}} = \alpha \Delta T \mathbf{I}$, where α is the coefficient of thermal expansion, ΔT is the temperature change and $\mathbf{I}$ is the identity matrix. The stress σ is then decomposed into volumetric and deviatoric parts as

$$\sigma_{\mathrm{vol}} = 3K_b \varepsilon^{\mathrm{e}}_{\mathrm{vol}} = \mathbf{I} : \sigma \tag{5.3}$$

$$\sigma_{\mathrm{dev}} = 2G \varepsilon^{\mathrm{e}}_{\mathrm{dev}} = \sigma - \sigma_{\mathrm{vol}} \tag{5.4}$$

where K_b and G are the bulk and shear modulus respectively and $\varepsilon^{\mathrm{e}}_{\mathrm{vol}}$ is the volumetric strain and $\varepsilon^{\mathrm{e}}_{\mathrm{dev}}$ the deviatoric strain.

Considering the significant thermomechanical loads encountered during service use of railway wheels, material yielding is unavoidable. The flow rule defining the plastic region is introduced via the von Mises yield criterion

$$f = \sqrt{\frac{3}{2} (\sigma_{\mathrm{dev}}) : (\sigma_{\mathrm{dev}})} - \sigma_{\mathrm{Y}} < 0 \tag{5.5}$$

where σ_{Y} is the initial yield stress. This is then further extended by noting that the material hardens both isotropically (yield surface expansion or contraction) and kinematically (moving yield surface to account for e.g. Bauschinger effect). This is accounted for by adding a term R and a back stress that shifts the origin in stress space by a vector $\mathbf{X}$ (back stress vector), giving the general flow rule used

$$f = \sqrt{\frac{3}{2} (\sigma_{\mathrm{dev}} - \mathbf{X}) : (\sigma_{\mathrm{dev} - \mathbf{X}})} - R - \sigma_{\mathrm{Y}} < 0 \tag{5.6}$$

During yielding, the plastic strain rate is then determined by using the previously introduced deviatoric stresses and back stresses

$$\dot{\varepsilon}^{\mathrm{p}} = \dot{\lambda}\frac{\partial f}{\partial \sigma} = \frac{\eta(f)}{t_*}\sqrt{\frac{3}{2}}\frac{\boldsymbol{\sigma}_{\mathrm{dev}} - \boldsymbol{X}}{|\boldsymbol{\sigma}_{\mathrm{dev}} - \boldsymbol{X}|} \tag{5.7}$$

where $\eta(f)$ is the determined overstress function controlling the viscoplastic behaviour, which is explained in detail in the coming subsection, and t^* is a calibration parameter controlling the behaviour.

The hardening is implemented in two different ways. The isotropic one is given by

$$\dot{R} = \dot{\lambda} b(Q - R) \tag{5.8}$$

which results in a function that saturates on Q (positive or negative value). The kinematic hardening is based upon the Chaboche decomposition of the Armstrong-Frederick rule [105, 106], together with a relaxation term and a thermodynamic term (usually omitted in practice due to the effect being relatively weak unless the temperature rate is significant)

$$\dot{\boldsymbol{X}}_i = \dot{\lambda}\left(\frac{2}{3}C_i\boldsymbol{\nu} - \gamma_i\boldsymbol{X}_i\right) - \frac{1}{\tau_i}\left(\frac{|\boldsymbol{X}_i|}{M_i}\right)\boldsymbol{X}_i + \frac{1}{C_i}\frac{dC_i}{dT}\dot{T}\boldsymbol{X}_i \tag{5.9}$$

$$\boldsymbol{X} = \sum_{i=1}^{i_{\max}} \boldsymbol{X}_i \tag{5.10}$$

To achieve a continuous curve in the plastic regime for different final strain levels (i.e. very low to very high plastic strains), it is suggested to use several components so that $i_{\max} = 3$ or 4, generally dependent on the stress and strain levels required for the specific scenario.

Finally, the hardness variation seen in Figure 4.6 is accounted for by the inclusion of a correction factor

$$H = H_{\mathrm{specimen}}/H_{\mathrm{ref}} \tag{5.11}$$

where 250 HV is the reference hardness as determined by previous experiments [88]. This is a non-standard addition compared to the normal Chaboche model, but required due to the hardness gradient in the wheel. From experimental observation, this is considered as a multiplicative factor to the yield stress and plastic moduli C_i. The radial hardness gradient in the wheel rim (and parts of the hub) is considered as linear in [28, 29, 72] and non-linear in [Paper E, Paper G], using a second-order polynomial fit to radial hardness data.

Viscoplastic model

Another aspect that is important to capture when modelling railway wheel steels of elevated temperatures is the *viscoplastic* behaviour of the material, i.e. how it relaxes for a given straining and how it depends on the loading *rate*. From experiments on railway steel similar to ER7 [117], it can be seen that the mechanical behaviour shows a strong dependence on the strain rate, stiffer response at higher rates. Performing tests at high strain rates, in particular cyclic tests, is however difficult due to the requirements on the setups [118]. Standard testing machines are generally not stiff enough for high loading rates, and specialised setups (Split Hopkinson bars or impact testers) do not produce results for cyclic loading.

A comparison of different overstress functions which provide the viscoplastic behaviour, is made in [106], where the markedly different behaviours are shown. In [95], which the current work is based upon, a Delobelle hyperbolic sine (sinh) is chosen. This has an almost constant exponent for low rates, and then a very high exponent at high strain rates, leading to a saturation of the viscous behaviour (i.e. the flow function f becomes almost constant at high strain rates).

The exact formulation used for the overstress function used in the present work is given as

$$\eta(f) = \sinh\left(\left\langle \frac{f}{D} \right\rangle^{n}\right) \tag{5.12}$$

where $\langle x \rangle$ denotes Macaulay brackets, giving x if $x \geq 0$ and 0 if $x < 0$. It should be noted that the material model is not calibrated against high-rate data, as no testing could be performed. The isothermal material calibration tests were performed at rates between 5×10^{-4} and 9×10^{-2} s^{-1} (the exact rate depends on the specific test). High strain rate behaviour in simulations is thus probably not accurate, due to it depending on values calibrated from rather low strain rate tests. This may be an issue for rolling contact test, where the strain rate is 10 to 100 s^{-1}.

Thermomechanical considerations

One of the important points of the thermomechanical problem is that all parameter variations should be à priori known functions of temperature. Different methods are available for this, in that the function can either be postulated as shown in [119] or be (linearly or non-linearly) interpolated between values determined at specific temperatures as in [95].

Because parts of the wheel can reach temperatures above 500 °C [28, 29] and knowledge that the strength of steel deteriorates significantly at these temperatures, this should be accounted for. In a previous study [95], this is considered through calibration using isothermal testing results at set temperature levels between 20 and 650 °C. In **Paper A** anisothermal results [89] are also introduced to improve the behaviour by finding a basis for material parameter variations that account for changing temperatures. Examples of the behaviour for several different temperatures and degrees of constraint (i.e. allowed percentage of thermal expansion) are shown in Figure 5.3.

Calibration using the anisothermal data captures material behaviour not seen in the isothermal tests, primarily the time-dependent degradation of the material. Due to the slow heating of the specimen during the isothermal tests, the spheroidisation of the material had already occurred and thus not visible in the data. Furthermore, any coupling between the isothermal temperature levels would not be visible but extrapolated, and thus could not be accounted for when calibrating the model.

As evidenced in other studies [88, 89, 94, 95], the pearlitic steel lamellar structure breaks down into spheroidised pearlite starting at around 450 °C. This process is accelerated at higher temperatures, showing very rapid deterioration at 600 °C. An example of spheroidisation is shown in Figure 5.4, with the broken lamellae encircled. The testing performed to characterise this is shown in Figure 5.5, with the curve showing the model behaviour included. Because of the relatively few cycles until failure at 1300 s, the onset of material damage is modelled rather than the more long-term thermal deterioration near failure. The decision was made to saturate the effect at a higher level than the experimental data would suggest due to this effect, as any crack growth might affect the behaviour. Furthermore, the reduction in hardness after the tests predicts a smaller reduction than the one applied here, which also suggested other weakening effects than thermal.

The formulation used for modelling damage is similar to the one used for isotropic hardening, and a similar model for softening has been suggested previously in [93]. The rate of the thermal degradation P is determined by

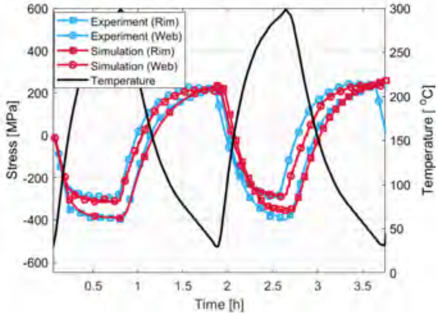

(a)

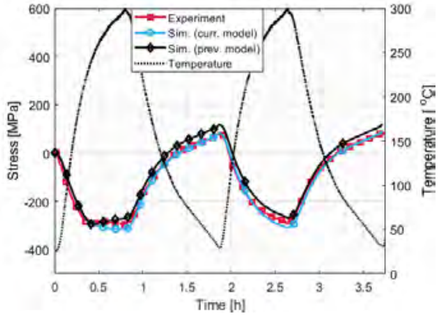

(b)

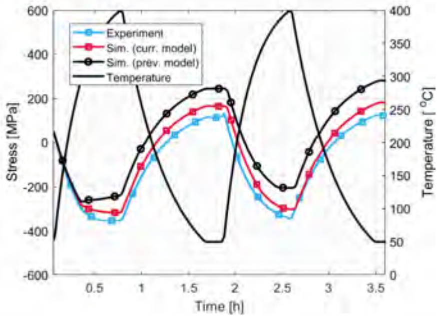

(c)

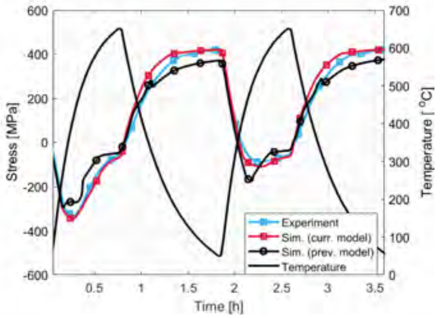

(d)

Figure 5.3: Anisothermal experiments in blue compared to the FE simulation results, in red for the **Paper A** model and black (for b, c and d) for the model from [95], for (a) 300 °C at full expansion constraint, (b) 300 °C at 50% thermal expansion constraint, (c) 400 °C at 50% thermal expansion constraint, (d) 650 °C at 50% thermal expansion constraint.

$$\dot{P} = \rho(P_\infty - P) \tag{5.13}$$

.

where ρ is a rate parameter and P_∞ is the saturation level, both temperature-dependent parameters. These are then applied to the yield stress and tangential moduli. Furthermore, because of the low strain rates seen during the anisothermal cycling, it was observed that the static relaxation introduced in Equation (5.9) generally overpowered the increase due to the loading. This behaviour was captured by adding a correction factor Λ

$$\dot{\boldsymbol{X}}_i = \dot{\lambda}\left(\frac{2}{3}C_i\boldsymbol{\nu} - \gamma_i\boldsymbol{X}_i\right) - \frac{\Lambda}{\tau_i}\left(\frac{|\boldsymbol{X}_i|}{M_i}\right)\boldsymbol{X}_i + \frac{1}{C_i}\frac{dC_i}{dT}\dot{T}\boldsymbol{X}_i \tag{5.14}$$

$$\Lambda = 1 - \frac{\langle\dot{T}\rangle}{|\dot{T}|} \tag{5.15}$$

This means that if there is still heating or cooling, static relaxation is prevented. Further improvements to this would include a threshold value rather than a binary state, but this was found sufficient for current needs.

5.3 Future improvements

The described material model has been shown to work relatively well when comparing the simulation results with experimental data for specimens and brake tests. It has also shown reasonable convergence behaviour in that it is able to reach a solution even when subject to significant contact loads, although the required time step is generally very small. This is a vast improvement as compared to previously employed generations of isothermally calibrated material models, which were quite unstable.

It can be questioned whether the current degree of complexity is necessary. For the loading scenario of rolling contact and braking, static relaxation is not generally required. This is because relaxation primarily occurs over relatively long time spans, compared to the rapid loading rate of rolling contact. In concurrence with this, the temperature-dependent kinematic hardening term seen in e.g. Equation (5.14) is generally low, which suggests that it may not be a significant addition. Previous work [92–95] has eschewed it for this reason. For typical values of C_i and its relevant change with respect to temperature,

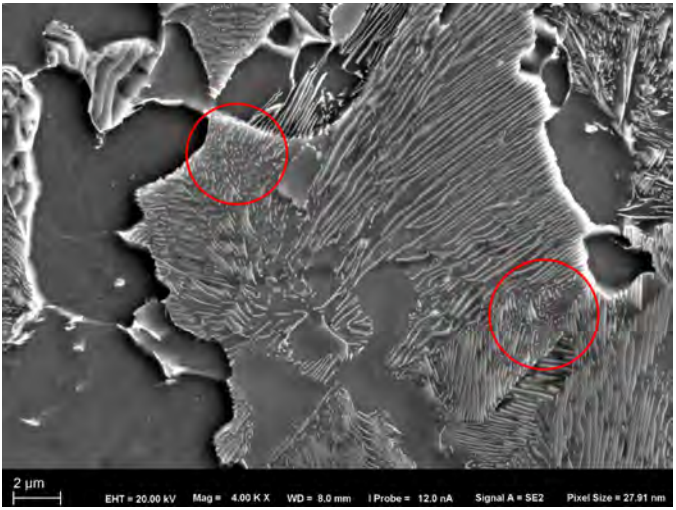

Figure 5.4: Spheroidisation of the pearlitic steel as shown using an electron microscope. Image courtesy of Erika Steyn.

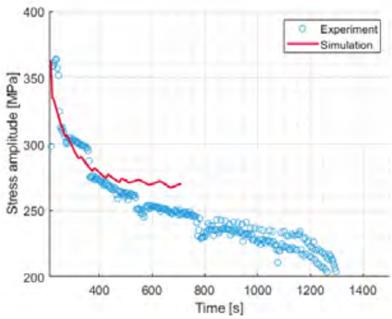

(a)

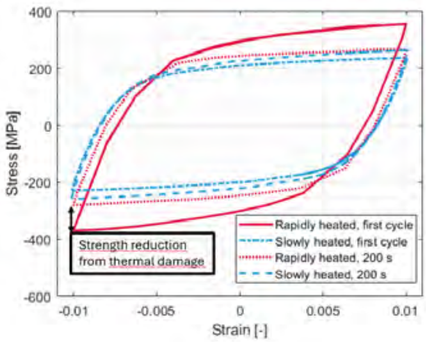

(b)

Figure 5.5: Thermal deterioration seen during rapid heating and then cycling at 600 °C. a) Stress amplitude at constant strain vs time, b) Stress-strain curves at two points in time comparing rapid and slow heating. Note that the slowly heated sample was pre-heated to 600 °C for several hours prior to testing.

this only affects the solution at very rapid heating rates such as high-power stop braking scenarios with very high pre-existing back stresses [19].

Several of the additions introduced in this work (hardness corrections, thermal deterioration) could be investigated in more detail, to better understand how to mimic difficult-to-describe phenomena, as well as to also improve the parameter values with more experimental data. Primarily, an anisothermal calibration in conjunction with the traditional isothermal calibration scheme may suggest better values or behaviours for these phenomena. Furthermore, calibration using data for significantly higher loading rates are likely necessary so that behaviour during typical contact loading scenarios can be modelled. Additionally, behaviour during scenarios including cracks [78] should be considered in future works.

Considering the high temperature levels measured during the tests, an investigation into including phase-transformation effects such as the models implemented in [120, 121]. It is not clear whether such high temperatures are reached in practice other than at the thermoelastic instabilities or contact interface, but considering some form of material change could nonetheless be of interest. This would incur a significant increase in model complexity, likely requiring some other simplification at first, but could nonetheless improve the modelling aspects of tread braking.

CHAPTER 6

Experimental testing

From the previous chapters, it has been seen that analytical and numerical solutions tend to be complicated and approximate. To study the full wheel-brake-rail system, and to provide data, experimental testing is required. This is a wide-encompassing term, as the experimental setups can range from universal testing machines and pin-on-disc testing, full-scale dynamometer test rigs to in-field measurements on trains in service.

As a major focus of this work has been on the improvement and verification of numerical models, data gathering and dissemination have been a fundamental aspect. To this end, experimental characterisation of the anisothermal behaviour of pearlitic steel, full-scale brake and rolling contact tests of wheels and field measurements of wheel temperatures have all been conducted. This is further augmented with results from previous experimental campaigns conducted within previous CHARMEC projects.

This chapter intends to detail the experiments conducted, and the setups used both for the testing conducted within the appended papers and to give an introduction to the various kinds of experiments performed at brake testing.

6.1 Full-scale laboratory testing

Full-scale testing entails the usage of actual wheels or wheelsets, with brake actuators or brake disc setups capable of providing enough braking power to fully decelerate inertial loads corresponding to individual wagons. These are often approximated by flywheels on the test axle. Other requirements may be to offer long-term braking as required by the EN standards. The need to mimic actual field service conditions results in large and expensive dynamometer setups with several tonnes of rotational mass, (concrete) foundations to prevent movement, power supply up to hundreds of kilowatts to a few megawatts, air ducting or water cooling as well as measurement systems to gather data. In addition, technical personnel will be required depending on the rules regarding the usage of the dynamometers. Most testing concerns brake friction material, as exemplified in UIC 541-4 [41], where appendix A concerning test programmes for composite brake blocks lists 164 steps, with an additional 57 for downhill braking. Wheel testing, where the wheel's resilience to service braking loads is evaluated, tends to be comparatively faster.

The benefit of these systems is that the conditions are, ideally, close to field conditions. The major discrepancies are mostly that only individual wheels, wheelsets or bogies are studied. Added benefits would be that it can be more precisely controlled, and more exact measurements can be made, as laboratory settings allow for instruments that would be difficult to mount on trains in service. The thermographic camera used in the testing in this project is an example of this. It has sensitive optics that would likely not last a very long in the rough conditions that are encountered under a train.

Two examples of brake rig designs have been used during this project. One custom design primarily intended for drag braking at Chalmers University has been used in **Paper C**, **Paper D** and **Paper F** to investigate the thermomechanical effects during both pure tread braking and when combined with rolling contact. An introduction to this brake roller rig, which has been developed during the course of the present work, is given in section 6.1. The other design is a more traditional type at RTRI, Tokyo, intended for both stop and drag braking with capabilities for high-speed testing. This rig has been used in **Paper F**, but also in papers from previous authors [19, 78, 81].

Chalmers Brake Roller Rig

The Chalmers Brake Roller Rig is an in-house designed testing rig used in the research in the present thesis. It was devised as a replacement and in several ways an improvement of an earlier rig, used in previous research conducted at CHARMEC, at Lucchini Surahammar, Sweden, presented in e.g. [27]. The idea was to have a compact and flexible brake test rig that fulfilled the following criteria after completion:

- Capable of drag braking testing for load cases up to and beyond the requirements in [11].
- Provide a setup for controlled rolling contact testing during tread brake application to the test wheel.
- Have a compact footprint and be viable to move in the future if lab circumstances change.
- Be flexible with regard to future instrumentation and possibility of complementary tests, such as particle emission testing.

Two photos of the brake roller rig are shown in Figure 6.1. The entire rig is at testing housed within a 20-foot container, but can be moved outside if modification work needs to be done, and additional access is required. The entire rig rests on a dozen truck air springs to provide vibration isolation.

The control software is custom-written in LabView and controls both the data gathering and the braking sequence (primarily braking power) via an NI CompactDAQ system and an associated computer. Several auxiliary measurement devices are connected to the CompactDAQ to give an overview presentation through the graphical user interface. The custom code allows for flexibility for changes compared to off-the-shelf solutions.

Power is provided by two electric motors, one at 100 kW and one at 160 kW, controlled via two electrical control cabinets. These are connected to the wheel axle and the rail-wheel axle with rubber belts to two pulley wheels, but can also be connected together to provide combined power to a single axle, if required, giving a maximum output of 260 kW if the rail module is not in use. The rotational mass (inertia) provided by the used flywheels is not large enough for stop braking tests, leading to premature stopping. The desired gradual deceleration could, however, possibly be mimicked through controlled deceleration if the initial speeds remain within available electric power limits.

BFC tread brake units (4th generation) provided by Wabtec Faiveley Nordic are mounted on a free-swinging arm, each providing a brake force between 0 and 50 kN (0–0.25 to 5 bar pneumatic pressure respectively). If a rail wheel is mounted, only one BFC unit can be used. If the rail wheel is removed, it is possible to use two units in a 2 Bg or 2 Bgu configuration. It is also straightforward to modify the setup for disc braking by adding brake calipers and a rotor, although some modifications would be required.

The test rig has in the present work been used for controlled testing at constant speeds. It has been used for experiments in the appended **Paper C**, **Paper D** and **Paper F**, with results also being used as a basis for work in **Paper E** and **G**.

6.2 Small-scale laboratory testing

A multitude of test rig designs are in use, which could be represented by the denomination "small-scale". In this work, they are grouped into two distinct categories. The first refers to general materials testing machines such as uniaxial testing machines or rotating disc machines. These are not specific to railways but rather used for material characterisation during specific loading conditions unrelated to individual fields. They are designed for accurate and well-controlled testing of standardised specimens, which can give high-resolution data on e.g. cyclic behaviour or wear in sliding contact, but the actual loading cases tend to be somewhat abstract due to limitations of the machines (uni- or biaxiality, contact ellipse sizes, specimen designs etc.).

In **Paper A**, an MTS 809 servo-hydraulic biaxial test frame equipped with induction heating was used for the stress-strain-temperature characterisation of ER7 wheel steel used in the overall work [72]. The machine is shown in Figure 6.2. The strain is measured by an MTS water-cooled extensometer and the temperature by two K-type thermocouples and an Optris PI 160 thermal camera. This type exemplifies the universal testing machine, wherein an electrical motor or hydraulic system applies a controlled force or displacement and possibly temperature for a specimen sample.

Another type which is relevant to the present work although not used in any of the papers are 'pin-on-disc' [122] or 'disc-on-disc' [16, 17] tribometers,

Figure 6.1: The Chalmers brake roller rig outside of the container, from two different views.

wherein the tribological behaviour of two bodies can be studied. This has been used previously in tread braking research, primarily for wear behaviour (pin-on-disc) [123–125] and material damage characterisation (disc-on-disc).

The main issue with this type of downsized test rigs is commonly noted as the *scale problem* [126]. An example is physical size, where length might scale linearly, but volume would scale cubically. Other non-linear effects suffer similarly. Several other examples from [127] are given in Table 6.1. Material phenomena such as spheroidisation may be diffusion-driven, with the material change process accelerating at elevated temperatures. Achieving field-condition temperature distributions with high temperatures at the rim and lower temperatures close to the hub may require different testing times, which will result in different material effects. Contact pressure induces a stress field which decreases with the distance from the contact zone, but this might nonetheless still represent significant fractions of the volume of smaller-scale structures. This complicates the study of some coupled phenomena but does provide a flexible and accurate investigation of others. It is possible to account for these issues, and several schemes exist.

More specialised, downscaled versions of full-scale test rigs are also available. The designs can vary quite significantly but can consist of one or more scaled-down wheelsets, suspension (with full bogies possible), rail or rail-wheel, motor, coupling mechanisms (for different wheelsets), braking system and frames for attachments and constraints. These types of machines are present at several institutes, with a wide range of usage scenarios. Stability and vibration analyses, modal analyses, testing of subsystems, load behaviour, model verification and more aspects are studied [126, 127]. These are intended for railway-related testing, where full-scale setups may not be economically or spatially feasible. They are generally more practical to use due to the lower footprint and power requirements, compared to the full-sized dynamometers, which may be very resource-intensive investments and require significant infrastructure beyond the actual wheelset and brake setup. Customisability is

Quantity	Time	Force	Stiffness	Contact patch ellipse
Scaling factor	$\phi_t = \sqrt{\phi_l}$	$\phi_F = \frac{\phi_\rho \phi_l^4}{\phi_t^2}$	$\phi_k = \phi_\rho \phi_l^2$	$\phi_e = (\phi_\rho \phi_l^4)^{1/3}$

Table 6.1: Examples of scaling factors, based upon the independent length and density scaling factors ϕ_l and ϕ_ρ as described in [127].

another benefit, as the designs themselves can vary depending on the desired phenomena to study. Ease of use and better controllability due to less revolving mass is another significant benefit. This type has seen wide adoption for railway research during the last century, because of the need to validate theory and investigate new designs.

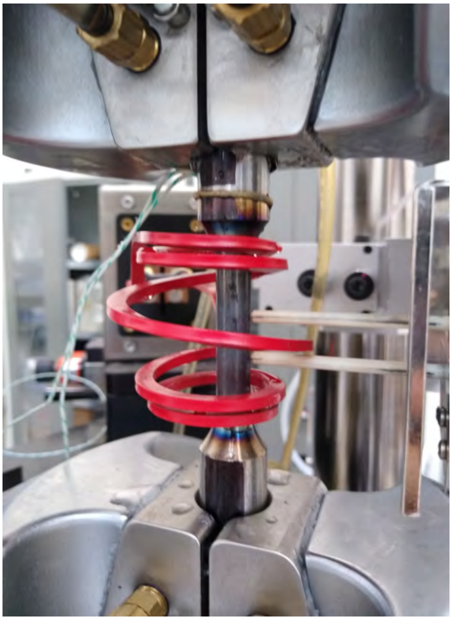

Figure 6.2: MTS 809 test frame with ER7 wheel steel specimen and induction coil.

One design that shows promise is the '4-point contact machine' [128], shown in Figure 6.3. In essence, it is a miniature brake roller rig that utilises both downscaled tread brakes and rail-wheels with nominally similar contact pressures and temperatures. Although the specific type of testing with 300 and 600 s duration tests is difficult to compare to full-scale results, it has shown qualitatively similar damage. It is still somewhat unclear how this type of machine compares to full-scale setups, but the results are promising.

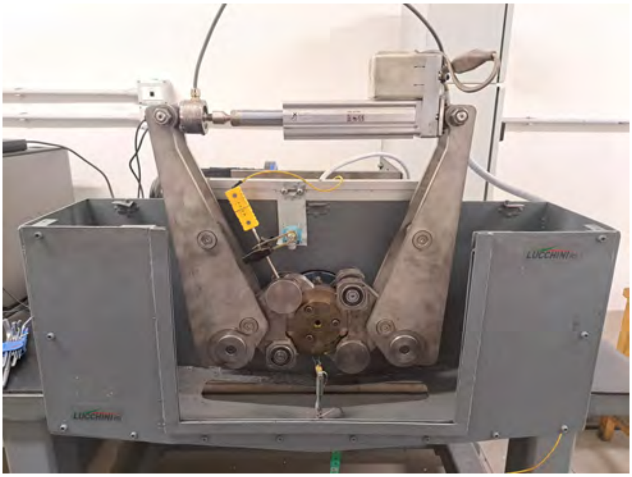

Figure 6.3: The 4-point contact machine in use at the University of Brescia. Photograph graciously provided by Mr Lorenzo Ghidini at Lucchini RS.

6.3 Field testing

Laboratory testing, full-scale or small-scale, are not true representations of the conditions in field, although many aspects can be closely mimicked. The railway industry requires that new technology is proven in full-scale field tests in representative conditions prior to implementation. Examples of this are given in e.g. [11] where procedures are listed for e.g. brake tests, testing of mechanical behaviour and acoustic field measurements, for new wheel designs. Field testing is problematic for several reasons, the primary one being cost. Closure of rail sections for sensor attachments or modifications to wagons in service requires cooperation of both infrastructure managers and train operators, both of which may have specific conditions or schedules. There are also practical difficulties with performing tests on running trains, as the undercarriage of a train is a rough environment, not suitable for sensitive equipment. Furthermore, the behaviour is not necessarily well-controlled compared to a lab where testing parameters can be set and maintained throughout a test whereas in field these can vary depending on rail and vehicle conditions, driver behaviour and many other factors. One example of unexpected issues is given in [129], where electrical disturbances interfered with the initial measurement set-up. However, many of these factors are also representing the benefits of field testing, as these variations in conditions are difficult to recreate in the laboratory.

Examples of brake field tests with vehicle-mounted equipment are given in [60, 129, 130]. In the former two, metro wheels and brake blocks were instrumented with thermocouples. In the third reference, a postal wagon was instrumented with a thermal camera to image the temperature field. Furthermore, other supplementary equipment such as data loggers to log data for speed, brake cylinder pressure, axle loads, GPS, acceleration. The temperature data was then used for calibration of numerical models.

More accessible alternatives are to perform the measurements, either by measuring on passing trains, as was done in [68] and in **Paper D**, the latter shown in shown in Figure 6.4, or by performing the measurements before and after scheduled tests [56, 131]. Preferably, a combination is used as several variables cannot be measured during the running sequence, such as residual stress field or material damage, whereas e.g. temperatures can only be measured during the test.

(a)

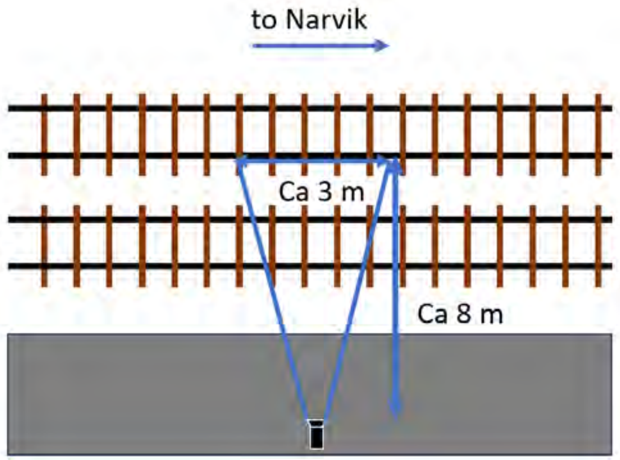

(b)

Figure 6.4: Field testing on the Ofoten line near Narvik (Norway). (a) Thermographic camera setup in Straumsnes. (b) drawing of the approximate position of the camera relative to the descending rail (furthest from the camera).

CHAPTER 7

Summary of Appended Papers

Paper A: Thermomechanical testing and modelling of railway wheel steel

In order to determine the thermomechanical behaviour of wheel steel during tread braking, a combined experimental and finite element study of ER7 wheel steel is performed. Thermomechanical specimen testing is performed for various combinations of anisothermal cycles and mechanical constraints designed to mimic actual brake cycles. Hardness testing is also performed to quantify material deterioration. These thermomechanical experiments combined with data obtained from previous isothermal experiments on the same material then form the basis for the calibration of a novel variant of a viscoplastic material model which includes a deterioration factor.

The results show good adherence to all anisothermal and isothermal loading cycles. The results also demonstrate that anisothermal testing and simulation is necessary to completely understand the material behaviour during thermomechanical loading.

Paper B: Improved modelling of tread braked wheels using an advanced material model

The objective is to investigate and examine the capabilities of a novel material model, calibrated using anisothermal and isothermal experimental data, when employed in detailed braking simulations corresponding to brake test rig conditions. To achieve this, an axisymmetric finite element model of a standard freight wheel exposed to tread braking is used. The finite element model accounts, in a simplified fashion, for residual stresses introduced by the rim hardening process at wheel manufacturing and also for variations in material properties based on typical hardness values for a wheel cross-section.

A range of braking situations are assessed to achieve different loads and temperatures, by mimicking downhill braking at constant speed for a prolonged time period. The results show that the anisothermally calibrated material model predicts substantially larger residual stresses compared to previous models. These new results compare better with real-world experience of wheel response to tread braking.

Paper C: Analysis and testing of tread braked railway wheel Effects of hot spots on wheel performance

To investigate the impact of localised heating phenomena in the form of hot spots on wheel performance in general and on wheel residual stress state in particular, a combination of experimental testing and finite element simulations of tread braked wheels has been performed. Using a newly established full-scale railway brake test rig, a wheel is exposed to prolonged drag braking applications at constant power levels to induce high temperatures on the wheel tread. The distribution and evolution of the temperature is studied using a high-speed, high-resolution thermographic camera in addition to traditional sliding thermocouples. Measured temperature data are then used in combination with a thermomechanically calibrated material model to simulate the wheel behaviour. For this purpose, a 3D finite element model representing a sector of a railway wheel is used.

The experimental results show that the temperatures measured utilising sliding thermocouples provide insufficient information since they cannot resolve the uneven tread temperatures given typical response times. Non-uniform heating is found to have a significant effect on tensile residual stresses in the rim. Especially the case with globally uneven temperatures is found to generate potentially hazardous residual stresses. The results present future challenges for the analysis and development of the brake-wheel-rail system.

Paper D: Characterisation and Evaluation of Global Uneven Heating during Railway Tread Braking – Brake Rig Testing and Field Study

An investigation and characterisation of the phenomenon of thermal localisation that can occur on tread braked railway wheels during prolonged braking is performed. This is done via a combination of full-scale laboratory tests and field measurements. Field testing is performed at the Swedish-Norwegian Iron ore line between Kiruna and Narvik, where the wheel temperatures were thermographically measured using a high frequency, high resolution thermographic camera. The laboratory testing is done at the brake test rig at Chalmers University in Gothenburg, with controlled testing at constant power level of three different types of railway freight wheels. The difference in intensity of the non-uniform temperature field as well as the incidence rate in service conditions and residual circumferential stress field were the primary quantities studied.

The results from this study show that long-wavelength non-uniform temperatures occurs on wheels in service use, primarily on wheels which are already significantly heated. The non-uniformity range is however smaller than in the laboratory measurements, likely due to the lower temperatures and higher cooling from the rail. The lab tests however show that there is a possibility of measurably increased residual stress levels due to the thermal localisation, compared to uniform heating.

Paper E: Non-uniform temperature and residual stress effects during railway tread braking

A numerical investigation of the thermomechanical phenomena arising due to global non-uniformities is performed. Experimental data from laboratory and field testing performed in **Paper D** is analysed to determine the behaviour of the non-uniform temperature field *during* tread braking. A heat flux model based on a Fourier series is then calibrated based on the temperature fields of the wheel treads at chosen time points during a test in the brake rig, utilising linear independence of the temperature modes for the terms of the series. The calibrated heat flux model and another model based on uniform heating are then used as input data into a thermomechanical simulation to calculate the differences in residual stress field.

The results from this study reinforce the conclusion from **Paper C** in that the non-uniform temperatures can have an impact on the average residual stress state in the wheel rim, comparable to a significant increase of the braking power. Furthermore, the thermal analysis and the calibration of the heat flux model show the complex behaviour of the non-uniform thermal flux, both spatially and temporally.

Paper F: Thermal Contact Behaviour of Tread Braked Wheels

Full-scale laboratory testing of tread braked wheels both with and without rolling contact is performed using two brake rigs. One for stop braking at RTRI in Japan and the other being the brake rig at Chalmers equipped with a new rail module for drag braking tests. Using high-speed radiometric techniques, the temperature field on the wheel rolling surface is measured to determine its behaviour during braking and rolling. Additionally, ultrasonic residual stress and crack measurements are performed on the stop braked wheels to study the mechanical effects of high-power stop braking for a commuter train case. Drag braking scenarios with rolling contact loading are then studied using the Chalmers brake rig in order to quantify the differences between the two types of braking.

The thermal contact behaviour between wheel and brake is shown for both sintered and organic composite brake blocks. Measured residual stress results at the wheel rim show that stop braking does not adversely affect the residual circumferential stress field compared to drag braking. Furthermore, cracks are shown to initiate after ca 40 stop braking tests from 110 km/h whereas none occur for drag braking for three tests at 20 to 40 kW with relatively low traction loads. Measurable wear at the rolling contact surface is however noted for the drag braking case.

Paper G: Numerical study of rolling contact during tread braking conditions

Finite element simulations of rolling contact are carried out, based on the testing performed in **Paper D**, **Paper F** and results from previous projects [19, 132] are performed. The simulations combine the material model from **Paper A** with rolling contact loading cases during both stop and drag braking. Compared to previous work on modelling rolling contact from the wheel point of view, contact interaction is used instead of precalculated contact stresses. Variations of temperature, rolling speed and contact force are studied. The influence of these variables on the damage state of the wheel is then evaluated to broaden the understanding of how the material model behaves during high loading rate scenarios.

The material model shows good convergence properties without instability during the simulations. Furthermore, an expected change in behaviour from elastic shakedown at low temperatures to significant ratchetting at high temperatures is observed. Although further calibration using high strain rate data is desirable, the material model shows promise for continued use in rolling contact simulations.

CHAPTER 8

Main Results and Conclusions

The aim of this thesis was to determine the limits of the tread braking system so that it can be utilised broadly in a safe and maintenance-efficient manner. This was then subdivided into three main focus areas: **extreme braking situations**, **temperature effects and rolling contact fatigue**, **wear of braking components**. To achieve this, finite element simulations of the braking and rolling contact scenarios with custom-made materials models were carried out. In parallel to this, extensive laboratory testing of steel specimens, full-scale brake roller rig testing and field measurements were accomplished. Although more could be said, the present work shows that the wheel is a quite resilient component of the railway system.

The main contributions of this thesis are:

- Material testing of the ER7 railway steel was conducted in **Paper A**. Specimens were tested anisothermally in thermomechanical loading cases designed to simulate the temperature and strain curves experienced by the wheel material in the wheel rim. The results from this shows that there is a significant effect of spheroidisation, i.e. breakdown of the pearlitic lamellae, on the mechanical strength of the steel.

- In **Paper A**, an existing material model calibrated for railway steel was extended to also account for temperature- and time-dependent effects. This model was calibrated to fit anisothermal and isothermal data. In **Paper B**, the model shows good results when compared to previously used models.

- In **Paper C**, the material model was used together with experimental results to calculate the effect non-uniform heating would have on the residual stress field in a railway wheel. It was shown that the normal thermoelastic instabilities had a negligible effect compared to uniform heating, but larger non-uniformities could be important. This was further studied in **Paper E**, with newly calibrated thermal results and better measurements of residual stresses on lab-tested wheels. In the latter paper, it was found that the history of the non-uniformities contribute significantly to the residual stress levels.

- The global non-uniformity of wheel temperatures was first seen in **Paper C** for one specific wheel, and then characterised in **Paper D** for several different wheels in the lab and several thousand in field.

- In **Paper E**, a characterisation of the non-uniformities found in **Paper D** was performed. Dominance of the long-wavelength modes and coupling between modes was shown. A finite element model of the non-uniform heating explored in **Paper D** was calibrated using a modal optimisation method. Good correspondence to experiment was shown, although a significant amount of modes was required.

- The temperature field during stop braking in a full-scale brake dynamometer is measured in **Paper F** for several different loading cases, indicating that the global non-uniformities are visible also for stop braking.

- Rolling contact experiments for an emergency braking case were performed in **Paper F**, exposing the wheel to more than a hundred emergency stop braking cycles to study the initiation and growth of the rolling contact fatigue cracks. It was found that the crack growth is generally quite mild compared to previous experimental results.

- Combined rolling contact and drag braking was also studied in **Paper F**, for a case of low tangential force. It was noted that RCF cracks did not form on the tread, although a measurable amount of wear was observed.

- The rolling contact behaviour of the material model was studied in **Paper G**, where simulations of braking scenarios from **Paper F** and [19] were used as a basis for the model. It was shown that the material model itself converges well for the contact loading cases, and that the behaviour is qualitatively reasonable.

CHAPTER 9

Future Work

Regarding the future, there are still significant amounts of work that can be performed in the field of railway tread braking. The work at our research centre that was started almost four decades ago is still ongoing, and likely will for the foreseeable future.

The material model introduced in **Paper A** and used in several other papers, although accurate for the cases it has been calibrated for still needs to be verified against other loading cases. This includes comparison to pure braking situations, with was partially studied in **Paper E**, fracture, fatigue and rolling contact. Although it is computationally stable and the results are reasonable in scope for the cases it was applied to in **Paper E** and **Paper G**, no comparisons to actual experimental data from full-scale testing was made apart from one consideration in **Paper E**.

Regarding the model itself, it is relatively well-known that the Chaboche model tends to misestimate ratcheting cases. This is solvable by the addition of, e.g. threshold terms [106] to the kinematic stress equations, but this also requires further calibration. The viscoplasticity is also an open question, as it is difficult to get accurate data for the strain rates experienced during rolling contact. Furthermore, much of the work has been hampered by the computational complexity, and it could be studied whether improvements in the efficiency of the current model could be made in order to lower computational time without overly affecting accuracy.

Similar issues could be raised about the thermal modelling. Some work has been performed in **Paper E** regarding the calibration of thermal models to mimic the resulting non-uniform temperature fields encountered. These efforts are predicted to continue for the near future in the **SD12** project. Still, solving the inverse problem, accounting for the nonlinear cooling (convection and radiation) and the thermal load resulting from the sliding contact, presents numerous opportunities for future studies.

The thermodynamical and thermomechanical side of braking would likely also need to be studied in greater detail. Although the experiments performed in the papers included in this thesis may generally answer what occurs temperature-wise during the tread braking process, *why* some phenomena such as thermal localisation occurs is not answered. Additional investigations into these phenomena may prevent damaging global non-uniform temperatures, which are difficult to detect in practice. The Chalmers brake roller rig has been equipped with a variable stiffness mounting for the BFC brake actuator unit, and future work will show whether this has an effect on the thermal behaviour of tread braking, including the occurrence of the thermal localisation.

Radiometric methods used in this thesis also present an area where more work can be done. Although the behaviours reported are believed to be accurate, radiometry is nonetheless a very sensitive method of measurement and is strongly influenced by the surface conditions, viewing angle and temperature of the material. Improved detection using e.g. two-colour methods, better knowledge of the surface conditions (in particular oxidation spots) and non-mirrored experimental setups would likely improve the data gained. Moreover, trackside hot wheel detectors would benefit from integration of multipoint temperature detectors or thermal cameras which would improve data from revenue traffic. This would help to identify problems regarding unevenly heated wheels.

The brake–roller–test rig at Chalmers University is also a likely candidate for future upgrades. Although functional for the drag braking scenarios envisioned using tread brakes, disc brakes are nonetheless also an important system to consider which could be included relatively painlessly. Furthermore, stop braking capacity through engine-controlled speed decrease to simulate brake actuator inertia could be of interest.

Finally, the greater goal would be to determine a holistic simulation model that can accurately predict wheel tread damage due to the effects discussed in the present thesis and more. This would likely entail significantly more testing at different loading conditions to gather the required data, as well as include novel methods to account for climate and geography, different braking strategies and influence of other primary and secondary methods of braking, wear of components, contact conditions and more. Many of these points are to be studied in the project **SD12**, which has recently commenced at CHARMEC. It is the author's hope that the present thesis will aid in this endeavour.

References

[1] EuroStat. “Freight transport statistics - modal split”. In: https://ec.europa.eu/eurostat/statistics-explained/index.php?title=Freight_transport_statistics_-_modal_split#Modal_split_of_freight_transport_in_the_EU.

[2] Su Chung and Won Young Lee. “Estimation of the Life-span for Urban Rolling Stock through LCC Analysis (Focused on Seoul Metro)”. In: *Journal of the Korean society for railway* 15 (Oct. 2012).

[3] LKAB. “Krisen på Malmbanan – LKAB tvingas dra ner produktionen”. In: https://lkab.com/press/krisen-pa-malmbanan-lkab-tvingas-dra-ner-produktionen/.

[4] NTSB. “Failed Wheel Bearing Caused Norfolk Southern Train Derailment in East Palestine, Ohio”. In: https://www.ntsb.gov/news/press-releases/Pages/NR20240625.aspx.

[5] The Japan Times. “Accident halts Tokaido Shinkansen services between Hamamatsu and Nagoya”. In: https://www.japantimes.co.jp/news/2024/07/22/japan/tokaido-shinkansen-halt/.

[6] LKAB. “Större axellast ökar kapaciteten på Malmbanan”. In: https://lkab.com/nyheter/storre-axellast-okar-kapaciteten-pa-malmbanan/.

[7] Evert Andersson et al. *Rail systems and rail vehicles*. KTH Railway Group, 2016.

[8] Central Japan Railway. "A braking system capable of safely stopping a train traveling at 311 mph". In: https://scmaglev.jr-central-global.com/about/emergency/.

[9] CHARMEC. "CHARMEC Research". In: https://www.charmec.chalmers.se/project.html.

[10] T. Vernersson. "Temperatures at railway tread braking. Part 1: Modelling". In: *IMechE: Journal of Rail and Rapid Transit* 221.2 (2007), pp. 167–182. ISSN: 09544097.

[11] CEN. *EN 13979-1 Railway applications - Wheelsets and bogies - Monobloc Wheels - Technical approval procedure - Part 1: Forged and rolled wheels.* Brussels (Belgium), 2023.

[12] CEN. *EN 13262 Railway applications - Wheelsets and bogies - Wheels - Product requirements.* Brussels (Belgium), 2020.

[13] Trafikverket. *Användning av bromsprocenttabeller m.m.* 2024.

[14] Trafikverket. *Beskrivning bromsprocenttabeller - Tågs bromsförmåga och relation till förbeskedsavstånd.* 2022.

[15] European Railway Agency. *Introduction to ETCS braking curves.* 2020.

[16] Angelo Mazzù et al. "Effect of shoe braking on wear and fatigue damage of various railway wheel steels for high speed applications". In: *Wear* 434-435 (2019), p. 203005. ISSN: 0043-1648.

[17] Michela Faccoli et al. "A Small-Scale Experimental Study of the Damage Due to Intermittent Shoe Braking on the Tread of High-Speed Train Wheels". In: *Tribology Transactions* 63.6 (2020), pp. 1041–1050.

[18] Michela Faccoli, Andrea Ghidini, and Angelo Mazzù. "Experimental and Numerical Investigation of the Thermal Effects on Railway Wheels for Shoe-Braked High-Speed Train Applications". In: *Metallurgical and Materials Transactions A* 49.10 (2018), pp. 4544–4554.

[19] Ali Esmaeili et al. "A methodology to predict thermomechanical cracking of railway wheel treads: From experiments to numerical predictions". In: *International Journal of Fatigue* 105 (2017), pp. 71–85. ISSN: 0142-1123.

[20] "Special Report: Rail freight transport in the EU: still not on the right track". In: European Court of Auditors, 2016.

[21] Duncan Dowson. *History of Tribology.* Wiley; 2nd edition, 1998.

[22] Hamilton Ellis. In: *Nineteenth Century Railway Carriages in the British Isles: from the Eighteen-thirties to the Nineteen-hundreds.* Modern Transport Publishing Co, 1949.

[23] Cable Car Museum. "Cable Cars: How they work - The Brakes". In: https://www.cablecarmuseum.org/the-brakes.html.

[24] U.S. Department of Transportation - Federal Railroad Administration. "Electronically Controlled Pneumatic Braking". In: (2017).

[25] Europe's Rail. "Digital Automatic Coupling - Delivery Programme". In: https://rail-research.europa.eu/latest-news/digital-automatic-coupling-dac-the-backbone-for-full-digital-rail-freight-train-operations-in-europe/.

[26] CEN. *EN 15313 Railway applications – In-service wheelset operation requirements – In-service and off-vehicle wheelset maintenance.* Brussels (Belgium), 2016.

[27] Daniel Thuresson. "Thermomechanics of block brakes". PhD thesis. Gothenburg: Chalmers Applied Mechanics, 2006.

[28] Eric Voortman Landström, Tore Vernersson, and Roger Lundén. "Analysis and testing of tread braked railway wheel — Effects of hot spots on wheel performance". In: *International Journal of Fatigue* 180 (2024), p. 108116. ISSN: 0142-1123.

[29] Eric Voortman Landström, Tore Vernersson, and Roger Lundén. "Characterisation and Evaluation of Global Uneven Heating during Railway Tread Braking – Brake Rig Testing and Field Study". In: *Chalmers Mechanics and Maritime Sciences* (2024).

[30] "JNS Procedure: Broken Wheels". In: ERA Joint Network Secretariat, 2019.

[31] T. Vernersson, M Peterson, and M. Hiensch. "Thermally induced roughness of tread braked railway wheels". In: *Proceedings 12th International Wheelset Congress.* Qingdao (China), 1998.

[32] "Directive 2001/16/EC of the European Parliament and of the Council of 19 March 2001 on the interoperability of the trans-European conventional rail system". In: *Official Journal of the European Union* (2001).

[33] "Directive 2002/49/EC of the European Parliament and of the Council of 25 June 2002 relating to the assessment and management of environmental noise - Declaration by the Commission in the Conciliation Committee on the Directive relating to the assessment and management of environmental noise". In: *Official Journal of the European Union* (2002).

[34] "Directive 2008/57/EC of the European Parliament and of the Council of 17 June 2008 on the interoperability of the rail system within the Community (Recast)". In: *Official Journal of the European Union* (2008).

[35] "Commission Decision of 4 April 2011 concerning the technical specifications of interoperability relating to the subsystem 'rolling stock – noise' of the trans-European conventional rail system (notified under document C(2011) 658)". In: *Official Journal of the European Union, 20112011/229/EU* (2011).

[36] "Commission Regulation (EU) No 1304/2014 of 26 November 2014 on the technical specification for interoperability relating to the subsystem 'rolling stock — noise' amending Decision 2008/232/EC and repealing Decision 2011/229/EU". In: *Official Journal of the European Union* (2014).

[37] Shahab Teimourimanesh. "Thermal Capacity of Railway Wheels - Temperatures, residual stresses and fatigue damage with special focus on metro applications". PhD thesis. Gothenburg: Chalmers Applied Mechanics, 2014.

[38] T. Vernersson. "Temperatures at railway tread braking. Part 2: Calibration and numerical examples". In: *IMechE: Journal of Rail and Rapid Transit* 221.4 (2007), pp. 429–441. ISSN: 09544097.

[39] Daniel Thuresson. "Influence of material properties on sliding contact braking applications". In: *Wear* 257.5 (2004), pp. 451–460. ISSN: 0043-1648.

[40] Tore Vernersson and Roger Lundén. "Wear of brake blocks for in-service conditions—Influence of the level of modelling". In: *Wear* 314.1 (2014). Proceedings 9th International Conference on Contact Mechanics and Wear of Rail / Wheel Systems, Chengdu, 2012, pp. 125–131. ISSN: 0043-1648.

[41] "Composite brake blocks - General conditions for certification and use". In: *UIC Report 541-4* (2018).

[42] SVT. "Efter järnvägsbränderna: Det finns brandsäkra tågbromsar som inte används". In: https://www.svt.se/nyheter/lokalt/vasternorrland/efter-jarnvagsbranderna-det-finns-brandsakra-tagbromsar-som-inte-anvands.

[43] SVT. "Trafikverket slår ifrån sig: Bromsarna är problemet". In: https://www.svt.se/nyheter/inrikes/trafikverket-om-kritiken-bromsarna-ar-problemet.

[44] A. TUDOR and M. M. KHONSARI. "Analysis of Heat Partitioning in Wheel/Rail and Wheel/Brake Shoe Friction Contact: An Analytical Approach". In: *Tribology Transactions* 49.4 (2006), pp. 635–642.

[45] Th.A. Dow and R.A. Burton. "Thermoelastic instability of sliding contact in the absence of wear". In: *Wear* 19.3 (1972), pp. 315–328. ISSN: 0043-1648.

[46] M. V. Korovchinski. "Plane-Contact Problem of Thermoelasticity During Quasi-Stationary Heat Generation on the Contact Surfaces". In: *Journal of Basic Engineering* 87.4 (Dec. 1965), pp. 811–817. ISSN: 0021-9223.

[47] R.C Parker and P.R. Marshall. "The measurement of the temperature of sliding surface with particular reference to railway brake blocks". In: *Proceedings Institution of Mechanical Engineers* 158 (1948), pp. 209–229.

[48] J. R. Barber. "Thermoelastic Instabilities in the Sliding of Conforming Solids". In: *Proceedings Royal Society of London. Series A, Mathematical and Physical Sciences* 312.1510 (1969), pp. 381–394. ISSN: 00804630.

[49] R.A. Burton, V. Nerlikar, and S.R. Kilaparti. "Thermoelastic instability in a seal-like configuration". In: *Wear* 24.2 (1973), pp. 177–188. ISSN: 0043-1648.

[50] Kwangjin Lee and J. R. Barber. "Frictionally Excited Thermoelastic Instability in Automotive Disk Brakes". In: *Journal of Tribology* 115.4 (Oct. 1993), pp. 607–614. ISSN: 0742-4787.

[51] Jr. Kennedy F. E. and F. F. Ling. "A Thermal, Thermoelastic, and Wear Simulation of a High-Energy Sliding Contact Problem". In: *Journal of Lubrication Technology* 96.3 (July 1974), pp. 497–505. ISSN: 0022-2305.

[52] Barber J. R. Yi Yun–Bo and Zagrodzki P. "Eigenvalue solution of thermoelastic instability problems using Fourier reduction". In: *Proc. R. Soc. Lond. A.4562799–2821* 456 (Aug. 2000), pp. 2799–2821.

[53] P. Zagrodzki et al. "Nonlinear Transient Behavior of a Sliding System With Frictionally Excited Thermoelastic Instability ". In: *Journal of Tribology* 123.4 (Jan. 2001), pp. 699–708. ISSN: 0742-4787.

[54] Przemyslaw Zagrodzki. "Thermoelastic instability in friction clutches and brakes – Transient modal analysis revealing mechanisms of excitation of unstable modes". In: *International Journal of Solids and Structures* 46.11 (2009), pp. 2463–2476. ISSN: 0020-7683.

[55] Georg-Peter Ostermeyer and Matthias Graf. "Influence of wear on thermoelastic instabilities in automotive brakes". In: *Wear* 308.1 (2013), pp. 113–120. ISSN: 0043-1648.

[56] T. Vernersson. "Thermally induced roughness of tread-braked railway wheels part 2: modelling and field measurements". In: *Wear* 236 (1999), pp. 106–116.

[57] Antonio Papangelo and Michele Ciavarella. "Can Wear Completely Suppress Thermoelastic Instabilities?" In: *Journal of Tribology* 142.5 (Feb. 2020), p. 051501. ISSN: 0742-4787.

[58] A. Papangelo and M. Ciavarella. "The effect of wear on ThermoElastic Instabilities (TEI) in bimaterial interfaces". In: *Tribology International* 142 (2020), p. 105977. ISSN: 0301-679X.

[59] Francis E. Kennedy. "Thermal and thermomechanical effects in dry sliding". In: *Wear* 100.1 (1984), pp. 453–476. ISSN: 0043-1648.

[60] Mandeep Singh Walia et al. "Performance of solid and segmented railway brake discs - temperature, wear and fatigue investigated by field experiments and simulations". In: *Chalmers Mechanics and Maritime Sciences (paper in thesis)* (2019).

[61] A.E. Anderson and R.A. Knapp. "Hot spotting in automotive friction systems". In: *Wear* 135.2 (1990), pp. 319–337. ISSN: 0043-1648.

[62] Coby L. Davis, Charles M. Krousgrill, and Farshid Sadeghi. "Effect of Temperature on Thermoelastic Instability in Thin Disks". In: *Journal of Tribology* 124.3 (May 2002), pp. 429–437. ISSN: 0742-4787.

[63] Kwangjin Lee and J. R. Barber. "Frictionally Excited Thermoelastic Instability in Automotive Disk Brakes". In: *Journal of Tribology* 115.4 (Oct. 1993), pp. 607–614. ISSN: 0742-4787.

[64] Dejian Meng et al. "Research on the evolution of friction hot spots in vehicle disc brake during braking based on experiment". In: *International Journal of Thermal Sciences* 203 (2024), p. 109126. ISSN: 1290-0729.

[65] P. Dufrénoy and D. Weichert. "A thermomechanical model for the analysis of disc brake fracture mechanisms". In: *Journal of Thermal Stresses* 26.8 (2003), pp. 815–828.

[66] S. Panier, P. Dufrénoy, and D. Weichert. "An experimental investigation of hot spots in railway disc brakes". In: *Wear* 256.7 (2004), pp. 764–773. ISSN: 0043-1648.

[67] Maurice Godet. "The third-body approach: A mechanical view of wear". In: *Wear* 100.1 (1984), pp. 437–452. ISSN: 0043-1648.

[68] John Cookson et al. "Tread damage due to extreme thermal localization under high braking loads in heavy haul operations". In: *Proceedings 20th International Wheelset Congress*. Chicago, IL (USA), 2023.

[69] Kazuyuki Handa and Fumiko Morimoto. "Influence of wheel/rail tangential traction force on thermal cracking of railway wheels". In: *Wear* 289 (2012), pp. 112–118. ISSN: 0043-1648.

[70] Becorit GmbH. "Datasheet Becorit 929-1". In: Recklinghausen, Germany, 1999.

[71] voestalpine. "zentrak hot box detection zentrak hot wheel detection". In: (2024).

[72] Eric Voortman Landström et al. "Thermomechanical testing and modelling of railway wheel steel". In: *International Journal of Fatigue* 168 (2023), p. 107373. ISSN: 0142-1123.

[73] *DEBBIE User's Manual*. Debro UMS, Warsaw, Poland, 1996.

[74] Anders Ekberg, Bengt Åkesson, and Elena Kabo. "Wheel/rail rolling contact fatigue – Probe, predict, prevent". In: *Wear* 314.1 (2014). Proceedings 9th International Conference on Contact Mechanics and Wear of Rail / Wheel Systems, Chengdu, 2012, pp. 2–12. ISSN: 0043-1648.

[75] A. Ekberg. "7 - Fatigue of railway wheels". In: *Wheel–Rail Interface Handbook*. Ed. by R. Lewis and U. Olofsson. Woodhead Publishing, 2009, pp. 211–244. ISBN: 978-1-84569-412-8.

[76] Anders Ekberg and Elena Kabo. "Fatigue of railway wheels and rails under rolling contact and thermal loading—an overview". In: *Wear* 258.7 (2005). Contact Mechanics and Wear of Rail/Wheel Systems, pp. 1288–1300. ISSN: 0043-1648.

[77] Kazuyuki Handa, Yoshisato Kimura, and Yoshinao Mishima. "Surface cracks initiation on carbon steel railway wheels under concurrent load of continuous rolling contact and cyclic frictional heat". In: *Wear* 268.1 (2010), pp. 50–58. ISSN: 0043-1648.

[78] Sara Caprioli, Tore Vernersson, and Anders Ekberg. "Thermal cracking of a railway wheel tread due to tread braking–critical crack sizes and in fluence of repeated thermal cycles". In: *Proceedings Institution of Mechanical Engineers, Part F: Journal of Rail and Rapid Transit* 227.1 (2013), pp. 10–18.

[79] Meysam Naeimi et al. "Thermomechanical analysis of the wheel-rail contact using a coupled modelling procedure". In: *Tribology International* 117 (2018), pp. 250–260. ISSN: 0301-679X.

[80] Katsuyoshi Ikeuchi et al. "Wheel tread profile evolution for combined block braking and wheel–rail contact: Results from dynamometer experiments". In: *Wear* 366-367 (2016). Contact Mechanics and Wear of Rail / Wheel Systems, CM2015, August 2015, pp. 310–315. ISSN: 0043-1648.

[81] Kazuyuki Handa, Katsuyoshi Ikeuchi, and Fumiko Morimoto. "Temperature-dependent wear of tread-braked railway wheels". In: *Wear* 452-453 (2020), p. 203265. ISSN: 0043-1648.

[82] R.G. Bayer. *Wear analysis for engineers*. New York, NY (USA): HNB Publishing, 2002.

[83] F. Braghin, S. Bruni, and R. Lewis. "6 - Railway wheel wear". In: *Wheel–Rail Interface Handbook*. Ed. by R. Lewis and U. Olofsson. Woodhead Publishing, 2009, pp. 172–210. ISBN: 978-1-84569-412-8.

[84] J.F. Archard. "Contact and rubbing of flat surfaces". In: *Journal of Applied Physics* 24 (1953), pp. 981–88.

[85] Mandeep Singh Walia. "Mechanical braking systems for trains". PhD thesis. Gothenburg: Chalmers Mechanics and Maritime Sciences, 2019.

[86] J Kalousek and E Magel. "Achieving a balance: the "magic" wear rate". In: *Railway Track & Structures* 93 (1997), pp. 50–52.

[87] A. Ghidini, M. Diener, and J. Schneider. *Wheels for freight cars: development and applications for heavy haul service*. Lucchini RS, 2010.

[88] Dimitrios Nikas, Johan Ahlström, and Amir Malakizadi. "Mechanical properties and fatigue behaviour of railway wheel steels as influenced by mechanical and thermal loadings". In: *Wear* 366-367 (2016), pp. 407–415.

[89] Erika Steyn and Johan Ahlström. "Thermo-mechanical response of near-pearlitic steel heated under restriction of thermal expansion". In: *Journal of Materials Research and Technology* 32 (2024), pp. 1714–1724. ISSN: 2238-7854.

[90] T. Vernersson and R. Lundén. "Temperatures at railway tread braking. Part 3: Wheel and block temperatures and the influence of rail chill". In: *IMechE: Journal of Rail and Rapid Transit* 221.4 (2007), pp. 443–454. ISSN: 09544097.

[91] S. Teimourimanesh, R. Lundén, and T. Vernersson. "Braking capacity of railways wheels - state-of-the-art survey". In: *Proceedings 16th International Wheelset Congress*. Cape Town (South Africa), 2010.

[92] R. Brommesson and M. Ekh. "Experiments and modelling of the cyclic behaviour of Haynes 282". In: *Technische Mechanik* 32.2 (2012), pp. 130–145.

[93] R. Brommesson and M. Ekh. "Modelling of cyclic behaviour of Haynes 282 at elevated temperatures". In: *Materials at High Temperatures* 31.2 (2014). ISSN: 09603409.

[94] Ali Esmaeili et al. “High temperature tread braking simulations employing advanced modelling of wheel materials”. In: *Proceedings International Heavy Haul Association Conference*. Sydney (Australia), 2015.

[95] Ali Esmaeili et al. “Modelling of temperature and strain rate dependent behaviour of pearlitic steel in block braked railway wheels”. In: *Railway Engineering Science* 29.4 (2021), pp. 362–378. ISSN: 26624745.

[96] Mandeep Singh Walia et al. “Thermomechanical capacity of wheel treads at stop braking: A parametric study”. In: *International Journal of Fatigue* 113 (2018), pp. 407–415. ISSN: 01421123.

[97] H. Blok. “Theoretical study of temperature rise at surfaces of actual contact under oiliness lubricating conditions”. In: *The Institution of Mechanical Engineers, Proceedings General Discussion on Lubrication and Lubricants* 2 (1937), pp. 222–235.

[98] J. C. Jaeger. “Moving sources of heat and the temperatures at sliding surfaces”. In: *Journal and Proceedings Royal Society of New South Wales* 66 (1942), pp. 203–224.

[99] T. P. Newcomb. “Transient temperatures attained in disk brakes”. In: *British Journal of Applied Physics* 10.7 (1959), pp. 339–340.

[100] T. P. Newcomb. “Temperatures reached in a bimetallic brake drum”. In: *British Journal of Applied Physics* 11.9 (1960), pp. 445–447.

[101] T. P. Newcomb. “Temperatures reached in disc brakes”. In: *Journal of Mechanical Engineering Science* 2.3 (1960), pp. 167–177.

[102] Tore Vernersson. “Tread braking of railway wheels - noise-related tread roughness and dimensioning wheel temperatures : field tests, rig measurements and numerical simulations”. PhD thesis. Gothenburg: Chalmers Applied Mechanics, 2006.

[103] Knut Andreas Meyer, Rostyslav Skrypnyk, and Martin Pletz. “Efficient 3d finite element modeling of cyclic elasto-plastic rolling contact”. In: *Tribology International* 161 (2021), p. 107053. ISSN: 0301-679X.

[104] Bo Wang et al. “Wheel tread temperature assessment and its impact on rolling contact fatigue under long-term braking conditions”. In: *Tribology International* 200 (2024), p. 110162. ISSN: 0301-679X.

[105] J. L. Chaboche. "Sur l'utilisation des variables d'état interne pour la description du comportementviscoplastique et de la rupture par endommagement". In: *Proc. Problemes non-linéaires de mecanique, Symposium franco-polonais* (1979), pp. 137–159.

[106] J. L. Chaboche. "A review of some plasticity and viscoplasticity constitutive theories". In: *International Journal of Plasticity* 24.10 (2008), pp. 1642–1693. ISSN: 07496419.

[107] AAR. *Manual of standards and recommended practices section G: wheels and axles.* Washington (VA, USA), 2004.

[108] Roger Lundén. "Fatigue durability of tread-braked railway wheels - on admissible combinations of axle load, train speed and signalling distance". In: *IMechE Journal of Rail and Rapid Transit* 205.F1 (1991), pp. 21–33.

[109] Roger Lundén. "Contact region fatigue of railway wheels under combined mechanical rolling pressure and thermal brake loading". In: *Wear* 144.1-2 (1991), pp. 57–70.

[110] *Evaluation of Service-Induced Residual Stresses in Railroad Commuter Car Wheels.* Vol. Rail Transportation. ASME International Mechanical Engineering Congress and Exposition. Nov. 1998, pp. 25–31.

[111] Iker Irizar et al. "Temperature-dependent properties in thermomechanical simulation of railway wheels - Towards a test-free wheel design validation". In: *Proceedings 19th International Wheelset Congress.* Venice (Italy), 2019.

[112] G Donzella et al. "The effect of block braking on the residual stress state of a solid railway wheel". In: *Proceedings Institution of Mechanical Engineers, Part F: Journal of Rail and Rapid Transit* 212.2 (1998), pp. 145–158.

[113] "Definition of parameters for the thermomechanical calculation of wheels. Correlation between calculation and tests". In: *UIC Report B 169/RP17* (2005), pp. 1–25.

[114] C.O. Frederick and P.J. Armstrong. "A mathematical representation of the multiaxial Bauschinger effect". In: *Materials at High Temperatures* 24.1 (2007), pp. 1–26.

[115] Maysam Kiani and Gary T. Fry. “ Fatigue Analysis of Heavy-Haul Freight Railway Wheels ”. In: *Proceedings 20th International Wheelset Congress*. Chicago (IL, USA), 2022, pp. 47–54.

[116] Caroline Ansin et al. “ Simulation and Field Measurements of the Long-term Rail Surface Damage due to Plasticity, Wear and Surface Rolling Contact Fatigue Cracks in a Curve ”. In: *CM 2022 - 12th International Conference on Contact Mechanics and Wear of Rail/Wheel Systems, Conference Proceedings*. Melbourne (Australia), 2022, pp. 591–601.

[117] Lin Jing, Xingya Su, and Longmao Zhao. “The dynamic compressive behavior and constitutive modeling of D1 railway wheel steel over a wide range of strain rates and temperatures”. In: *Results in Physics* 7 (2017), pp. 1452–1461. ISSN: 2211-3797.

[118] ISO. “Metallic materials - Tensile testing at high strain rates - Part 1: Elastic-bar-type systems”. In: (2018).

[119] Hélène Morch et al. “Efficient temperature dependence of parameters for thermo-mechanical finite element modeling of alloy 230”. In: *European Journal of Mechanics, A/Solids* 85 (2021). ISSN: 09977538.

[120] Ali Esmaeili, Johan Ahlström, and Magnus Ekh. “ Modelling of cyclic plasticity and phase transformations during repeated local heating events in rail and wheel steels ”. In: *Proceedings - 11th International Conference on Contact Mechanics and Wear of Rail/Wheel Systems*. Delft (Netherlands), 2018, pp. 245–252.

[121] Björn Andersson. “Thermo-Mechanical-Metallurgical Modelling of Pearlitic Steels and Railhead Repair Welding”. PhD thesis. Gothenburg: Chalmers Industrial and Materials Sciences, 2024, p. 71.

[122] ASTM G99-04. *Standard Test Method for Wear Testing with a Pin-on-Disk Apparatus*. Tech. rep. ASTM, 2017.

[123] Tore Vernersson et al. “Wear of railway brake block materials at elevated temperatures: pin-on-disc experiments”. In: *Eurobrake 2012*. 2012.

[124] Andrea Ghidini Michela Faccoli Nicola Zani and Candida Petrogalli. “Tribological Behavior of Two High Performance Railway Wheel Steels Paired with a Brake Block Cast Iron”. In: *Tribology Transactions* 65.2 (2022), pp. 296–307.

[125] Michela Faccoli et al. “Experimental and numerical investigation on the wear behavior of high performance railway wheel steels paired with various brake block materials under dry sliding conditions”. In: *Wear* 506-507 (2022), p. 204456. ISSN: 0043-1648.

[126] Alfred Jaschinski et al. “The Application of Roller Rigs to Railway Vehicle Dynamics”. In: *Vehicle System Dynamics* 31.5-6 (1999), pp. 345–392.

[127] Daniele Mario Fraschini. “Dynamic Modelling of the KTH Roller Rig”. MA thesis. KTH, Sweden, 2021.

[128] Lorenzo Ghidini et al. “An innovative small-scale testing procedure to study damage in shoe-braked wheels”. In: *Proceedings Institution of Mechanical Engineers, Part F: Journal of Rail and Rapid Transit* 238.4 (2024), pp. 414–426.

[129] Mandeep Singh Walia et al. “Temperatures and wear at railway tread braking: Field experiments and simulations”. In: *Wear* 440-441 (2019), p. 203086. ISSN: 0043-1648.

[130] Shahab Teimourimanesh, Tore Vernersson, and Roger Lundén. “Modelling of temperatures during railway tread braking: Influence of contact conditions and rail cooling effect”. In: *Proceedings Institution of Mechanical Engineers, Part F: Journal of Rail and Rapid Transit* 228.1 (2014), pp. 93–109. ISSN: 09544097.

[131] Joseph L Lanigan et al. “Field trials of a methodology for locomotive brake testing to assess friction enhancement in the wheel/rail interface using a representative leaf layer”. In: *Proceedings Institution of Mechanical Engineers, Part F: Journal of Rail and Rapid Transit* 235.9 (2021), pp. 1053–1064.

[132] Sara Caprioli et al. “Thermal cracking of railway wheels: Towards experimental validation”. In: *Tribology International* 94 (2016), pp. 409–420. ISSN: 0301-679X.